Supporting Information

Tambjamine alkaloids and related synthetic analogs: efficient transmembrane anion transporters

Paulina Iglesias Hernández,[b] Daniel Moreno,[a] Anatalia Araujo Javier,[b] Tomás Torroba,[b] Ricardo Pérez-Tomás,*[b] and Roberto Quesada*[a]

[a] *Departamento de Química, Facultad de Ciencias, Universidad de Burgos,09001 Burgos, Spain. E-mail: rquesada@ubu.es*
[b] *Department of Pathology and Experimental Therapeutics, Cancer Cell Biology Research Group, Universidad de Barcelona, Barcelona, Spain. E-mail: rperez@ub.edu*

General Procedures and Methods

Commercial reagents were used without any further purification. as received. NMR spectra were recorded in Varian Mercury-300 MHz and Varian Unity Inova-400 MHz spectrometers. Chemical shifts are reported in ppm with using residual solvent peak as reference, coupling constants are reported in Hz. High resolution mass spectra (HRMS) were recorded on a Micromass Autospec S-2 spectrometer using EI at 70eV. UV-visible recording were performed with a Varian, Cary 300 Bio UV spectrophotometer, in 1 cm UV cells. Fluorescence spectra were acquired using a Varian, Cary eclipse spectrophotometer, in 1 cm fluorescence cubettes. 4-Methoxy-2,2'-bipyrrole-5-carboxaldehyde was prepared as described.[1]

Synthesis of Tambjamine derivatives

Compounds **1**-**6** were synthesised using modifications of the previously reported method.[2] 4-Methoxy-2,2'-bipyrrole-5-carboxaldehyde (190 mg, 1 mmol,)[1] was mixed with the corresponding amine (1.3 mmol, 1.3 equivalents) in 10 mL of chloroform. 40 uL of acetic acid were added and the mixture stirred at 60 ºC until TLC showed disappearance of the staring material. The reaction mixture was diluted with 40 mL of dichloromethane and washed with HCl 1M (3 × 25 mL). The organic fraction was dried over Na_2SO_4 and the solvent evaporated to yield **1**-**6** as yellow solids.

(Z)-N-((3-methoxy-5-(1H-pyrrol-2-yl)-2H-pyrrol-2-ylidene)methyl)-2-methylpropan-1-amine, Tambjamine C (**1**).

Yield (88%). UV-Vis ($CHCl_3$): λ_{max} 415nm (ε = 60087 $M^{-1}cm^{-1}$)
^{1}H-NMR ($CDCl_3$, 300MHz): δ = 13.43 (s, br, 1H) , 10.61 (s, br, 1H), 9.35 (m, 1H), 7.23 (d, *J* = 14.8 Hz, 1H), 6.95 (m, 1H), 6.72 (m, 1H), 6.20 (m, 1H), 5.95 (m, 1H), 3.82 (s, 3H), 3.22 (t, *J* = 6.4, 2H), 1.94 (hp, *J* = 6.7 Hz, 1H), 0.95 (d, *J* = 6.7 Hz, 6H). ^{13}C-NMR ($CDCl_3$, 75 MHz): δ = 164.07, 142.40, 140.91(CH), 124.06 (CH), 122.85, 113.32(CH), 110.93 (CH), 110.81, 91.45 (CH), 58.75 (CH_2), 58.71 (CH_3), 29.73 (CH), 20.02 (CH_3). HRMS (EI) m/z calcd for [C14H19N3O] 245,1528; found: 245,1528.

(Z)-N-((3-methoxy-5-(1H-pyrrol-2-yl)-2H-pyrrol-2-ylidene)methyl)ethanamine, Tambjamine D (**2**)

Yield (86%). UV-Vis ($CHCl_3$): λ_{max} 415nm (ε = 41356 $M^{-1}cm^{-1}$)
^{1}H-NMR ($CDCl_3$, 300MHz): δ = 13.63 (s, br, 1H) , 10.59 (s, br, 1H), 9.46 (d, br, 1H), 7.36 (d, *J* = 15.0 Hz, 1H), 7.06 (m, 1H), 6.73 (m, 1H), 6.28 (m, 1H), 5.94 (m, 1H), 3.93 (s, 3H), 3.56 (m, 2H), 1.42 7.36 (t, *J* = 7.3 Hz, 3H). ^{13}C-NMR ($CDCl_3$, 75 MHz): δ = 163.95, 142.26, 140.22(CH), 123.92 (CH), 122.87, 113.19, 110.92 (CH), 110.90, 91.44 (CH), 58.69 (CH_3), 45.56 (CH_2), 15.60 (CH_3).
HRMS (EI) m/z calcd for [C12H15N3O] 217,1215; found: 217,1211

(Z)-N-((3-methoxy-5-(1H-pyrrol-2-yl)-2H-pyrrol-2-ylidene)methyl)-2-phenylethanamine, Tambjamine F (**3**)

Yield (90%). UV-Vis ($CHCl_3$): λ_{max} 417 nm (ε = 55625 $M^{-1}cm^{-1}$)

---

[1] K. Dairi, S. Tripathy, G. Attardo, J.-F. Lavallee, *Tetrahedron Lett.* **2006**, *47*, 2605.
[2] D. M. Pinkerton, M. G. Banwell, A. C. Willis, *Org. Lett.* **2007**, *9*, 5127.

^{1}H-NMR ($CDCl_3$, 300MHz): δ = 13.41 (s, br, 1H) , 10.59 (s, br, 1H), 9.51 (m, 1H), 7.22 (m, 5H), 7.05 (d, *J* = 14.8 Hz, 1H), 6.98 (m, 1H), 6.73 (m, 1H), 6.22 (m, 1H), 5.92 (m, 1H), 3.79 (s, 3H), 3.64 (dd, *J* = 13.5, 6.82 Hz, 2H), 3.00 (t, *J* = 7.3 Hz, 2H).^{13}C-NMR ($CDCl_3$, 75 MHz): δ = 164.14, 142.56, 140.48(CH), 137.30, 129.19 (CH), 129.01 (CH), 127.15 (CH), 124.19 (CH), 122.85, 113.48(CH), 111.05 (CH), 110.99, 91.49 (CH), 58.79 (CH_3), 52.49 (CH_2), 36.74 (CH_2).
MS (EI) m/z calcd for [C18H19N3O] 293,1528; found: 293,15

(Z)-N-((3-methoxy-5-(1H-pyrrol-2-yl)-2H-pyrrol-2-ylidene)methyl)dodecan-1-amine, BE-18591(**4**)

Yield (86%). UV-Vis ($CHCl_3$): λ_{max} 415 nm (ε = 48386 $M^{-1}cm^{-1}$)
^{1}H-NMR ($CDCl_3$, 300MHz): δ = 13.66 (s, br, 1H) , 10.60 (s, br, 1H), 9.44 (m, 1H), 7.33 (d, *J* = 15.0 Hz, 1H), 7.06 (m, 1H), 6.73 (m, 1H), 6.27 (m, 1H), 5.94 (m, 1H), 3.92 (s, 3H), 3.47 (m, 2H), 1.75 (m, 2H), 1.24 (br, 15H), 0.87 (t, *J* = 6.6 Hz, 3H).
^{13}C-NMR ($CDCl_3$, 75 MHz): δ = 163.53, 141.89, 140.16(CH), 123.60 (CH), 122.48, 112.82(CH), 110.52 (CH), 110.47, 91.00 (CH), 58.28 (CH_3), 50.76 (CH_2), 31.70 (CH_2), 30.08 (CH_2), 29.41 (CH_2), 29.36 (CH_2), 29.23 (CH_2), 19.14 (CH_2), 28.92 (CH_2), 26.30 (CH_2), 22.48 (CH_2), 13.94 (CH_3).
MS (EI) m/z calcd for [C22H35N3O] 357,2780; found: 357,27

(Z)-N-((3-methoxy-5-(1H-pyrrol-2-yl)-2H-pyrrol-2-ylidene)methyl)aniline (**5**)

Yield (91%). UV-Vis ($CHCl_3$): λ_{max} 465 nm (ε = 54333 $M^{-1}cm^{-1}$)
^{1}H-NMR ($CDCl_3$, 300MHz): δ = 13.61 (br s, 1H) , 11.07 (d, *J* = 14.2 Hz, 1H), 10.63 (s, br, 1H), 7.61 (d, *J* = 14.2 Hz, 1H), 7.26 (m, 4H), 7.01 (m, 1H), 6.76 (m, 1H), 6.21 (m, 1H), 5.95 (m, 1H), 3.86 (s, 3H).
^{13}C-NMR ($CDCl_3$, 75 MHz): δ = 165.47, 144.58, 138.60, 130.02 (CH), 129.96 (CH), 125.88 (CH), 125.34 (CH), 122.65, 117.17 (CH), 115.17 (CH), 113.60, 111.57 (CH), 92.40 (CH), 59.03 (CH).
HRMS (EI) m/z calcd for [C16H15N3O] 265,1215; found: 265.1208

(Z)-4-tert-butyl-N-((3-methoxy-5-(1H-pyrrol-2-yl)-2H-pyrrol-2-ylidene)methyl)aniline (**6**)

Yield (90%). UV-Vis ($CHCl_3$): λ_{max} 452 nm (ε = 68232$M^{-1}cm^{-1}$)
^{1}H-NMR ($CDCl_3$, 300MHz): δ = 13.67 (br s, 1H) , 11.13 (d, *J* = 14.3 Hz, 1H), 10.65 (s, br, 1H), 7.66 (d, *J* = 14.3 Hz, 1H), 7.34 (d, *J* = 8.3 Hz, 1H), 7.26 (d, *J* = 8.3 Hz, 1H), 7.03 (m, 1H),6.77 (m, 1H), 6.23 (m, 1H), 5.97 (s, 1H), 3.89 (s, 3H), 1.28 (s, 9H).
^{13}C-NMR ($CDCl_3$, 75 MHz): δ = 165.21, 149.36, 144.14, 136.16, 130.35 (CH), 126.91 (CH), 125.18 (CH), 122.73, 117.08 (CH), 114.86 (CH), 113.36, 111.47 (CH), 92.26 (CH), 58.98 (CH_3), 34.78 (CH_3).
HRMS (EI) m/z [M]+ calcd for [C20H23N3O] 321,1841; found:321,1844

Characterization data

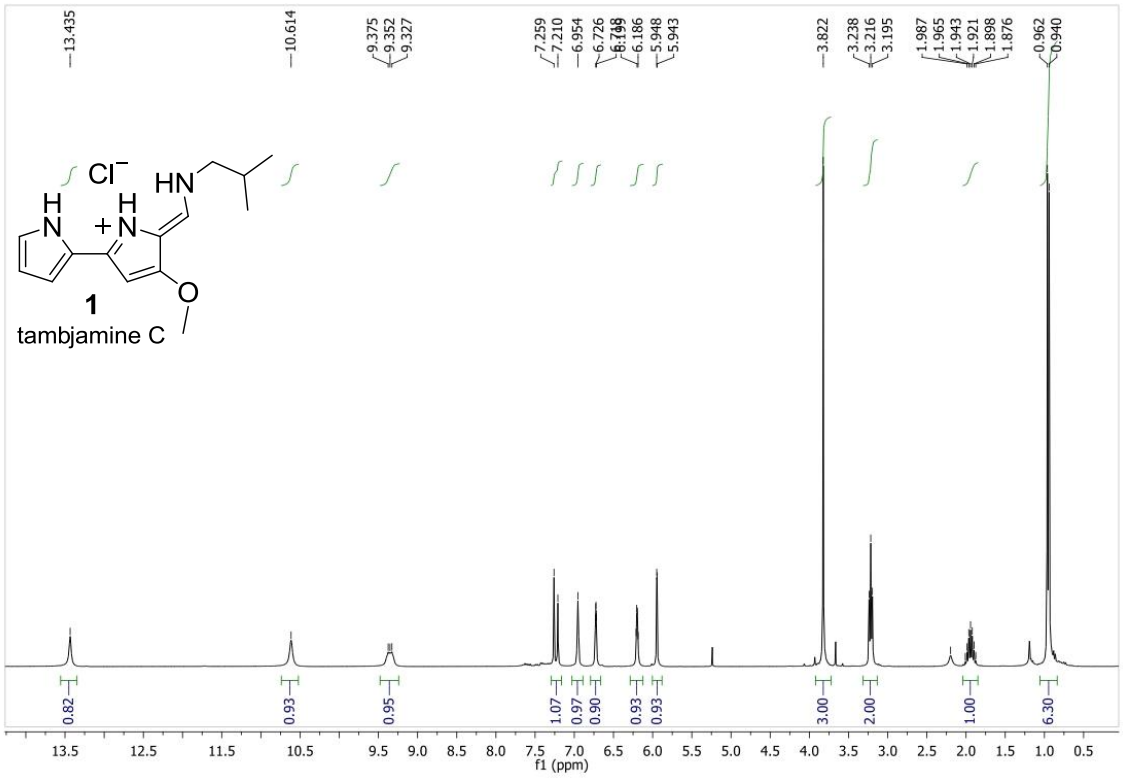

Figure S1. ^{1}H-NMR ($CDCl_3$, 300MHz) of compound **1**.HCl.

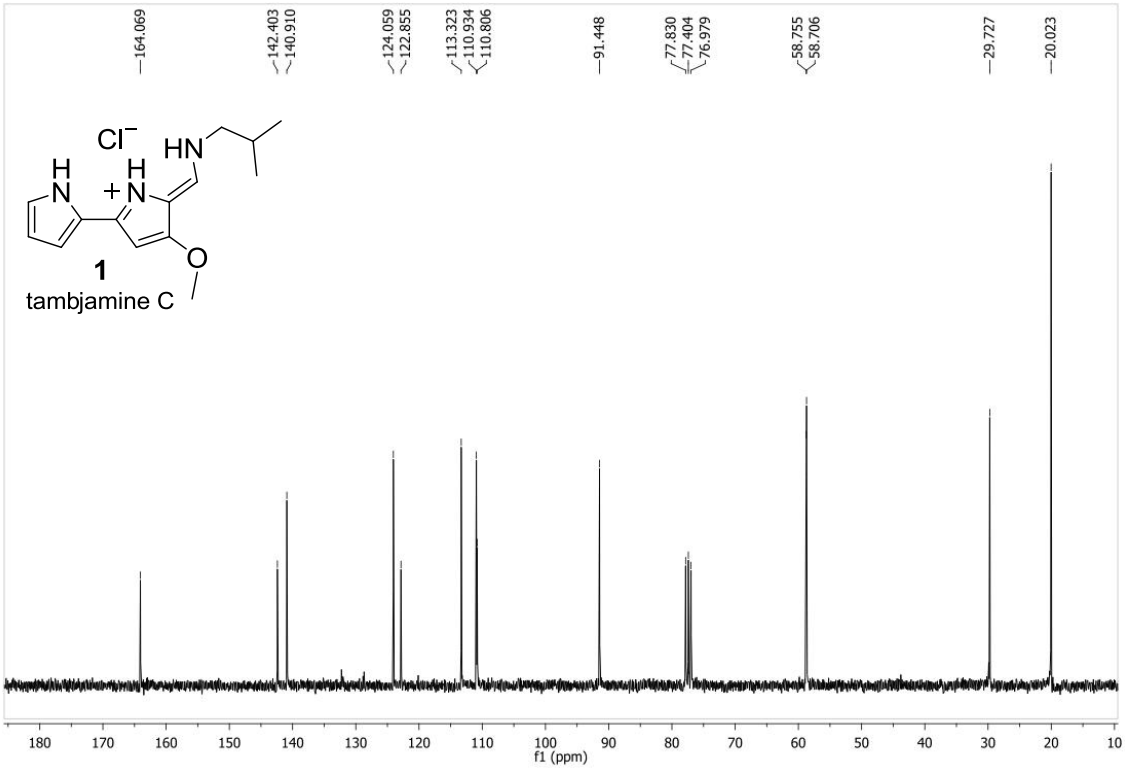

Figure S2. ^{13}C-NMR ($CDCl_3$, 75 MHz) of compound **1**.HCl.

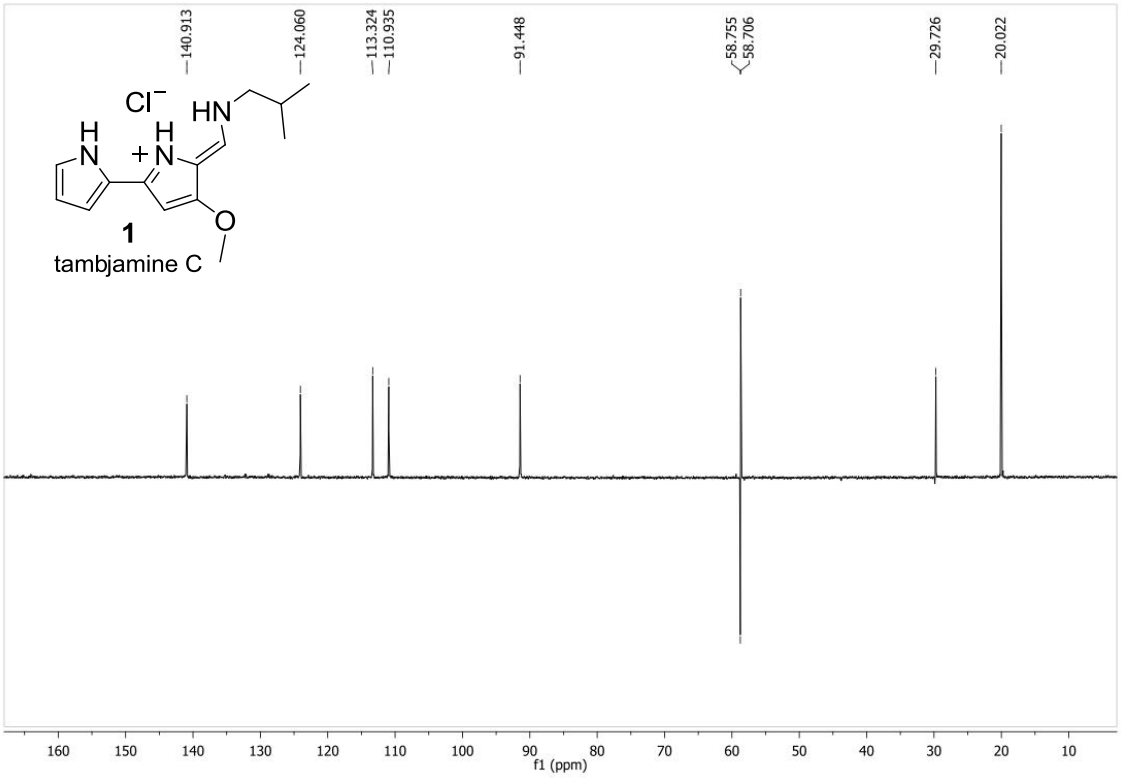

Figure S3. DEPT ^{13}C-NMR ($CDCl_3$, 75 MHz) of compound **1**.HCl.

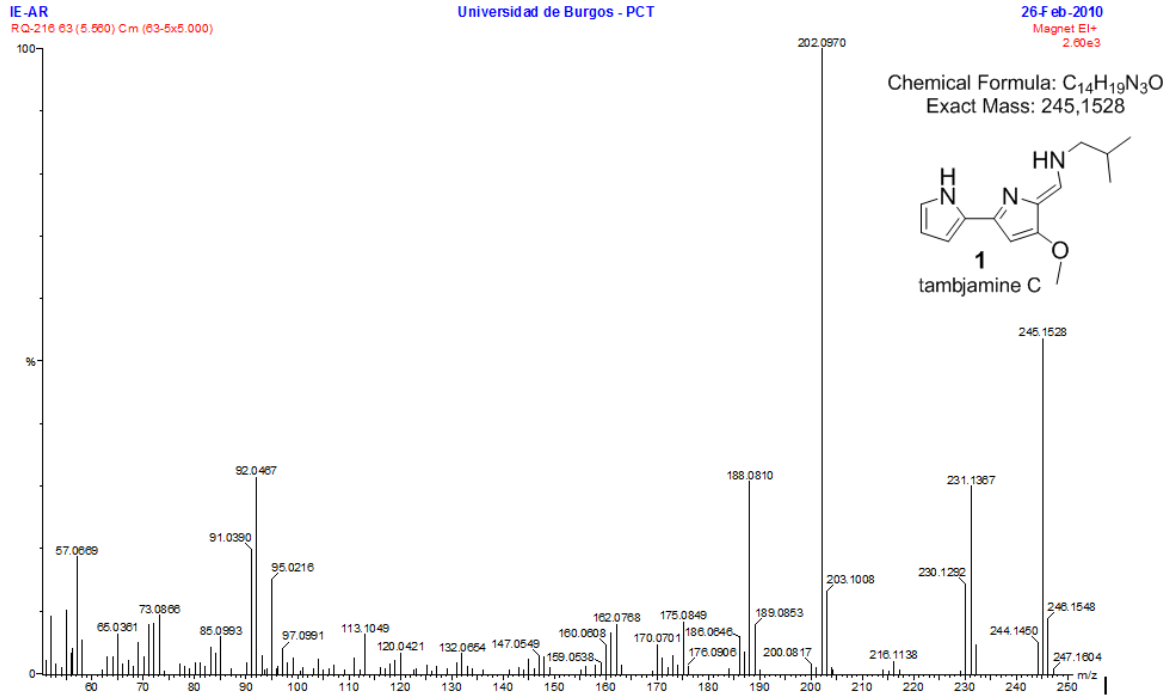

Figure S4. HRMS (EI) of compound **1**.

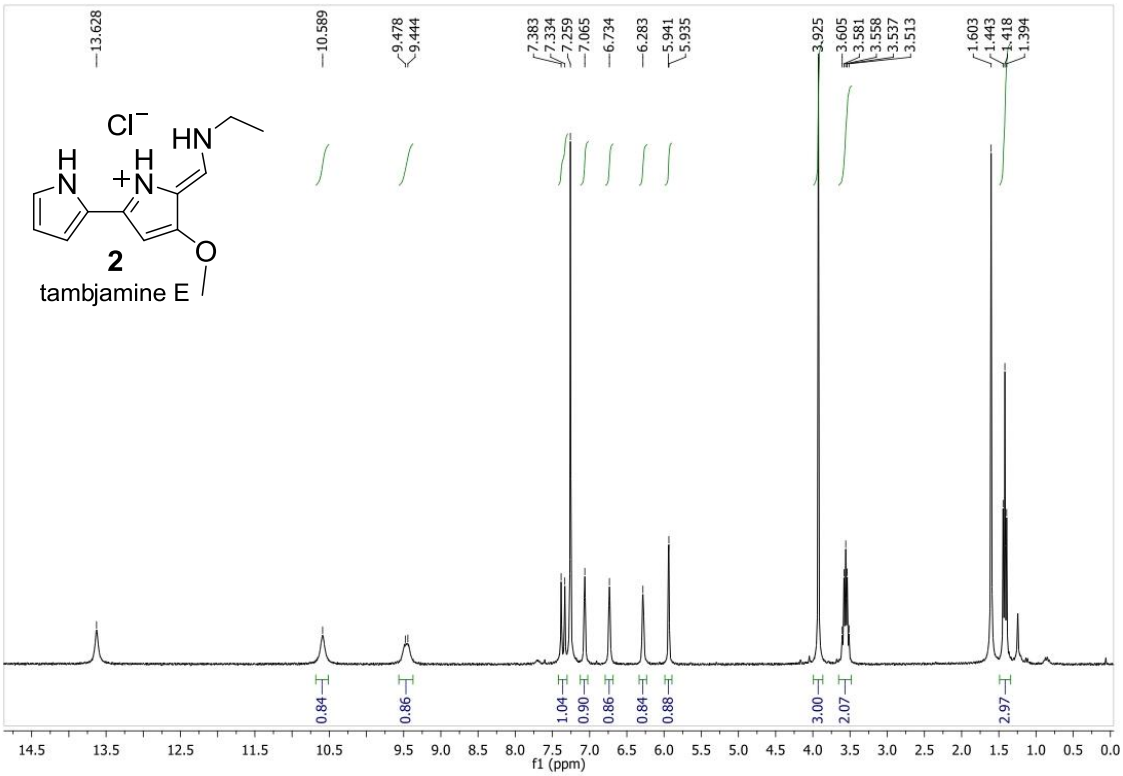

Figure S5. ^{1}H-NMR ($CDCl_3$, 300MHz)of compound **2**.HCl.

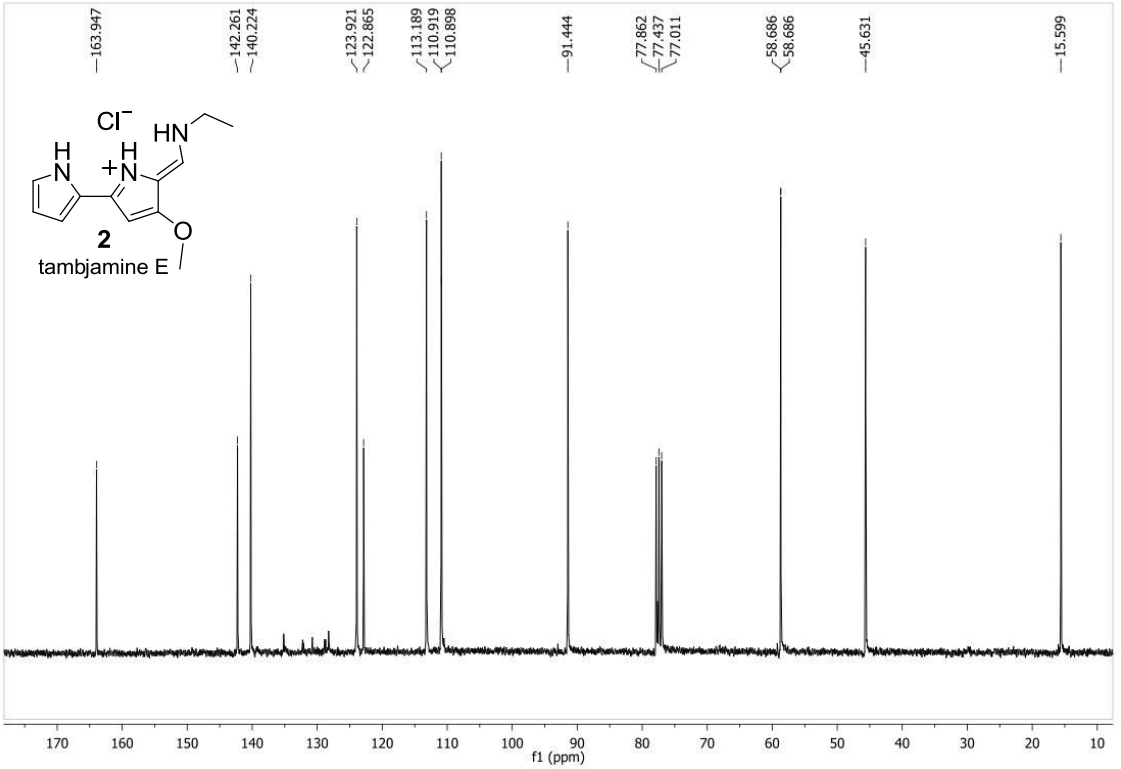

Figure S6. ^{13}C-NMR ($CDCl_3$, 75 MHz) of compound **2**.HCl.

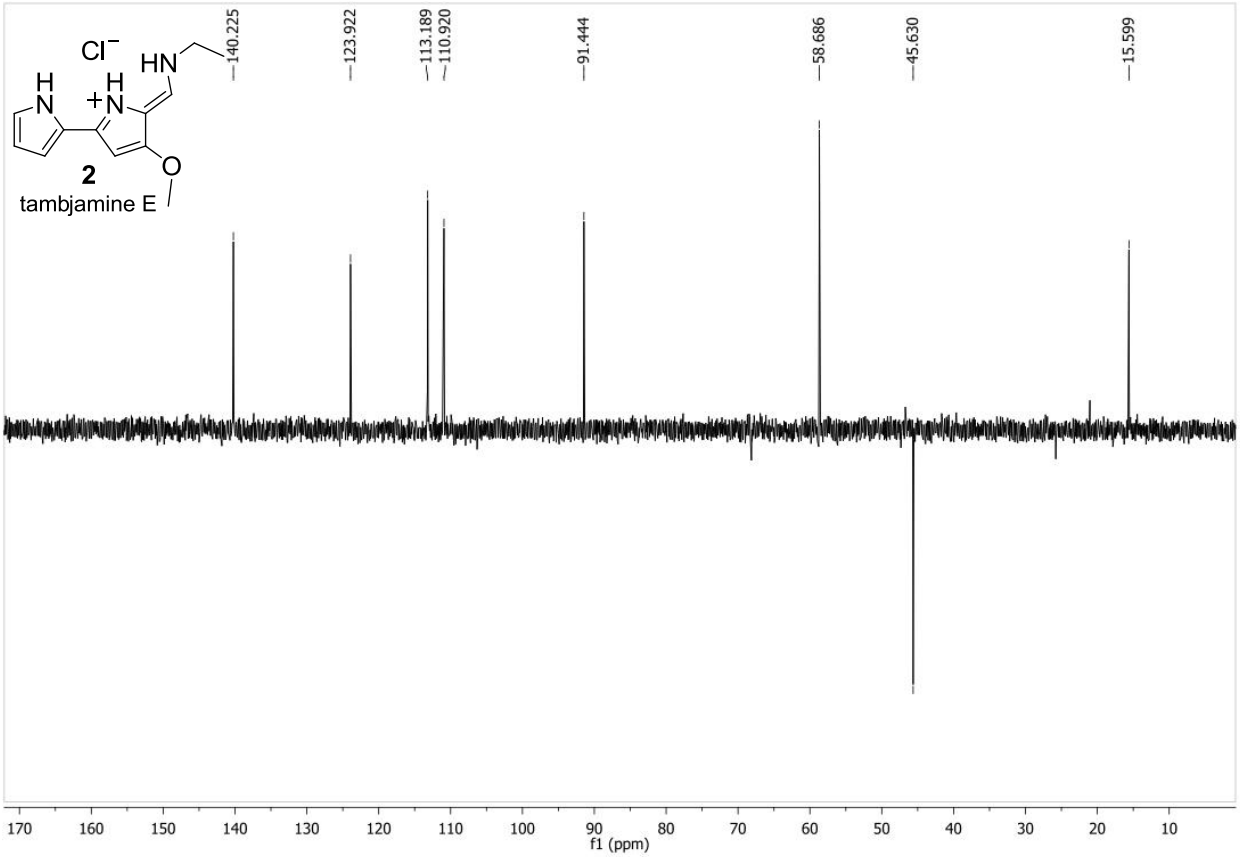

Figure S7. DEPT ^{13}C-NMR ($CDCl_3$, 75 MHz) of compound **2**.HCl.

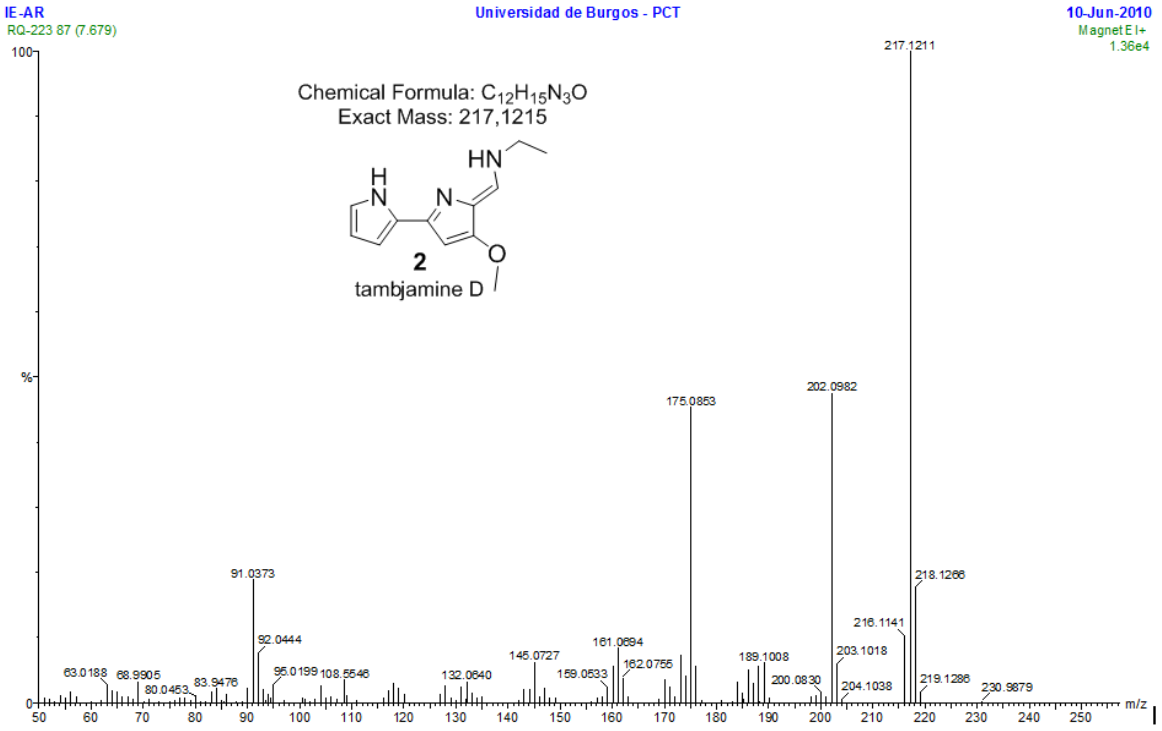

Figure S8. MS (EI) of compound **2**.

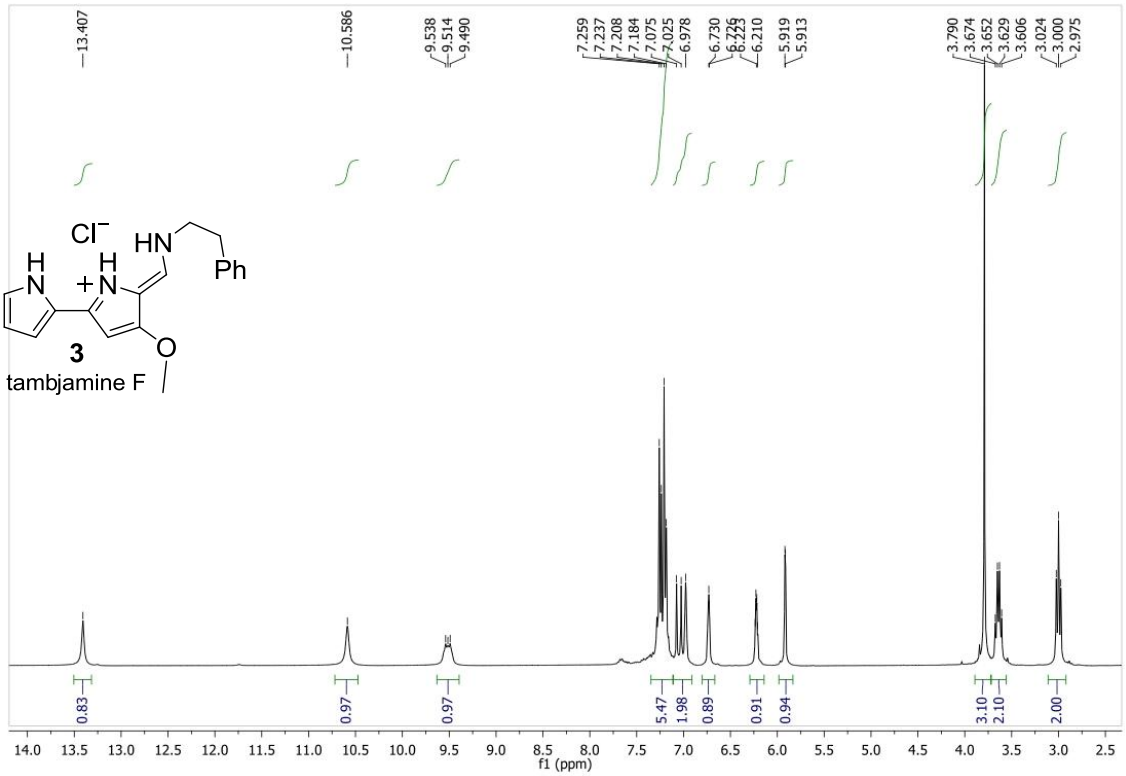

Figure S9. ^{1}H-NMR ($CDCl_3$, 300MHz) of compound **3**.HCl.

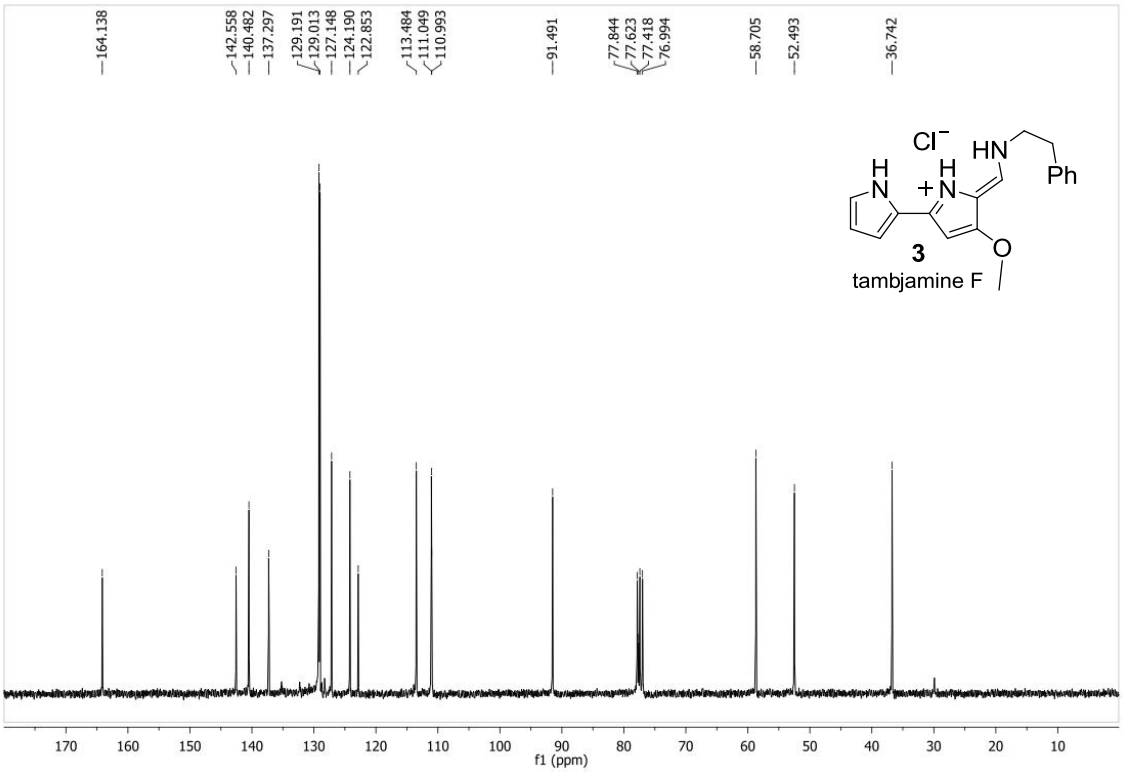

Figure S10. ^{13}C-NMR ($CDCl_3$, 75 MHz) of compound **3**.HCl.

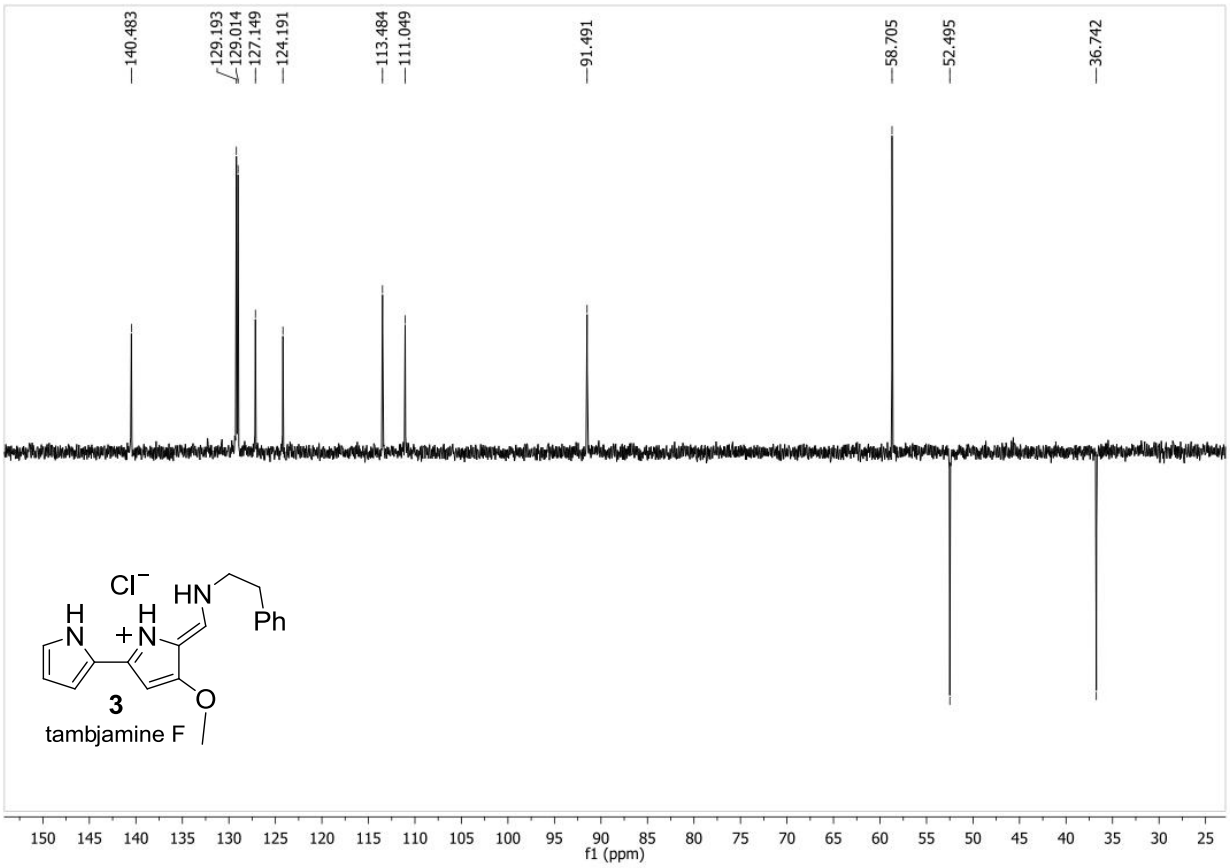

Figure S11. DEPT ^{13}C-NMR ($CDCl_3$, 75 MHz) of compound **3**.HCl.

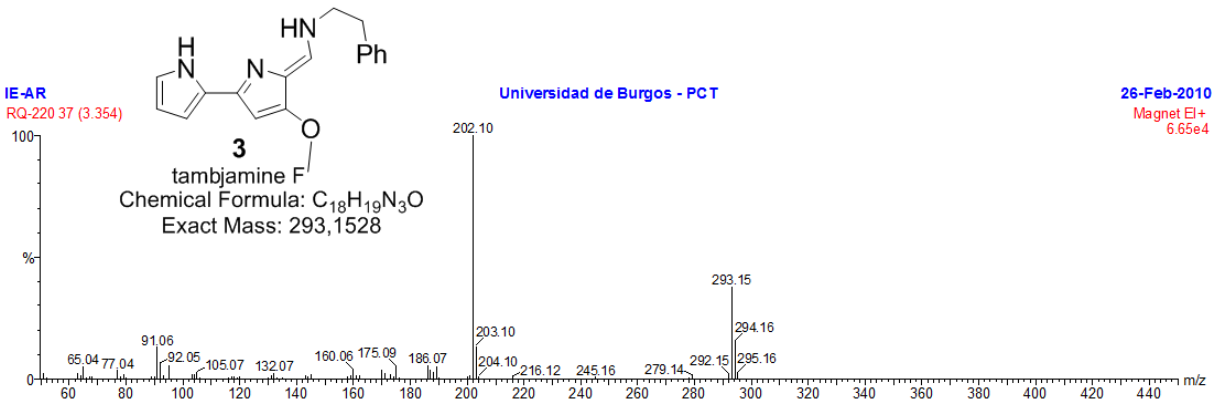

Figure S12. MS (EI) of compound **3**.

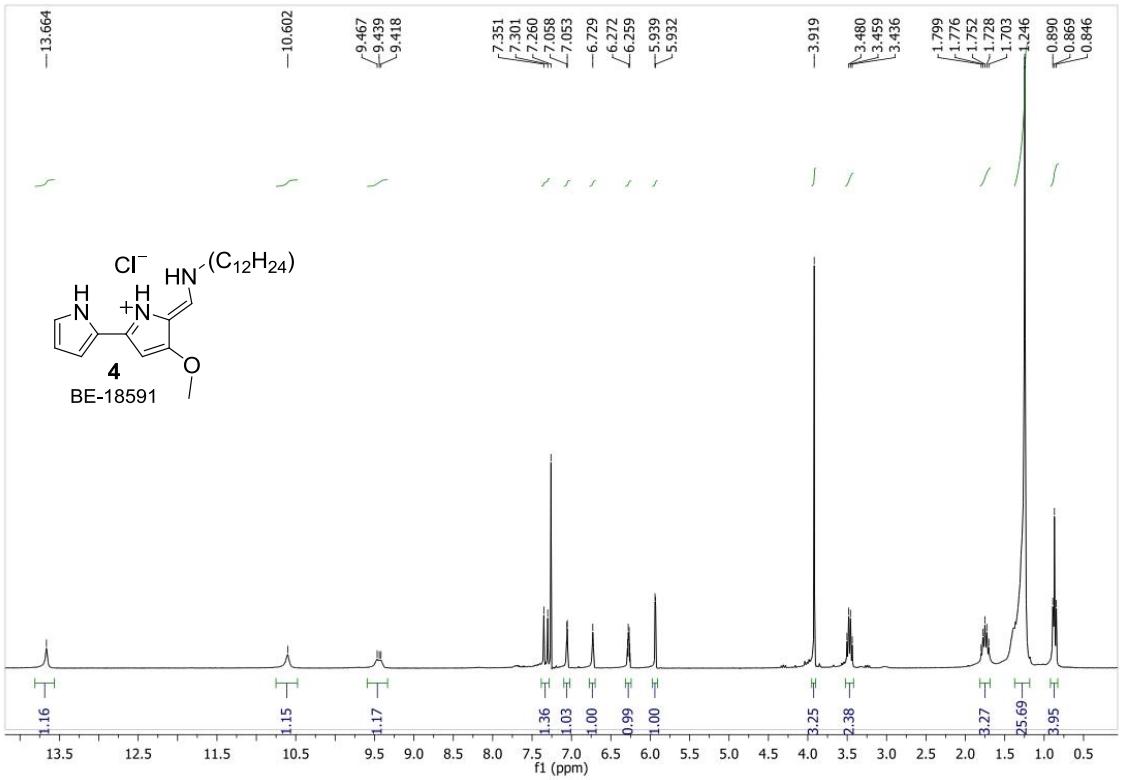

Figure S13. ^{1}H-NMR ($CDCl_3$, 300MHz) of compound **4**.HCl.

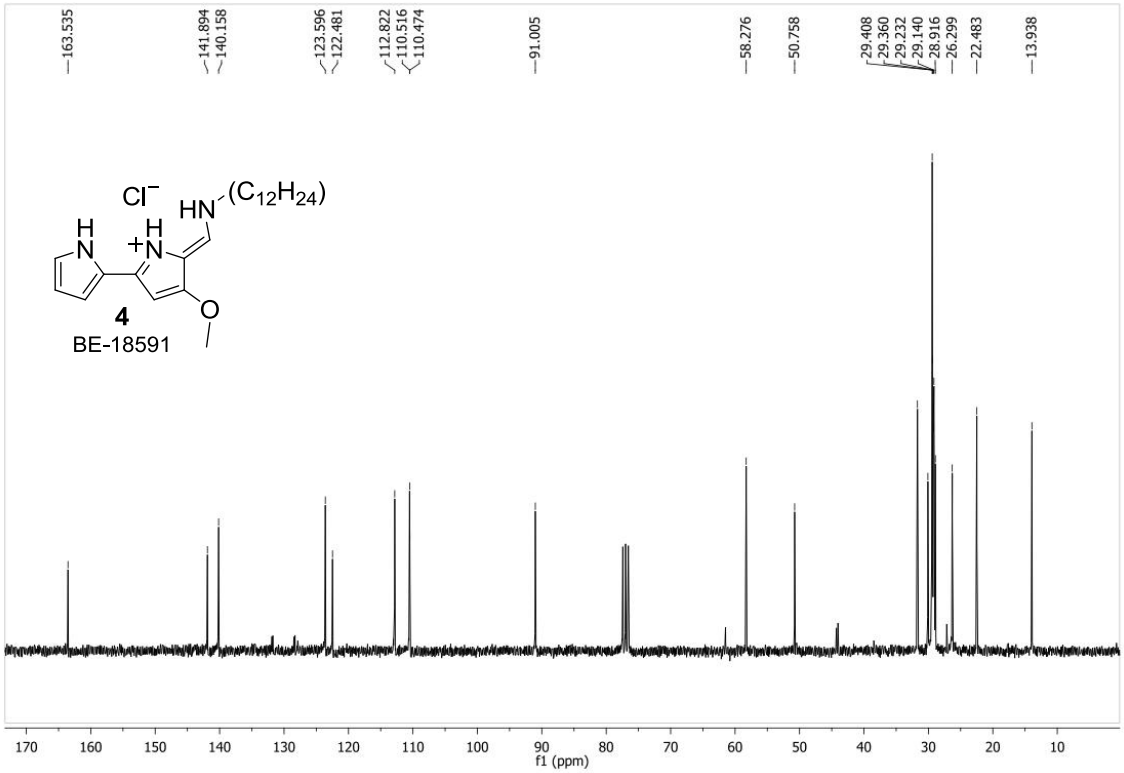

Figure S14. ^{13}C-NMR ($CDCl_3$, 75 MHz) of compound **4**.HCl.

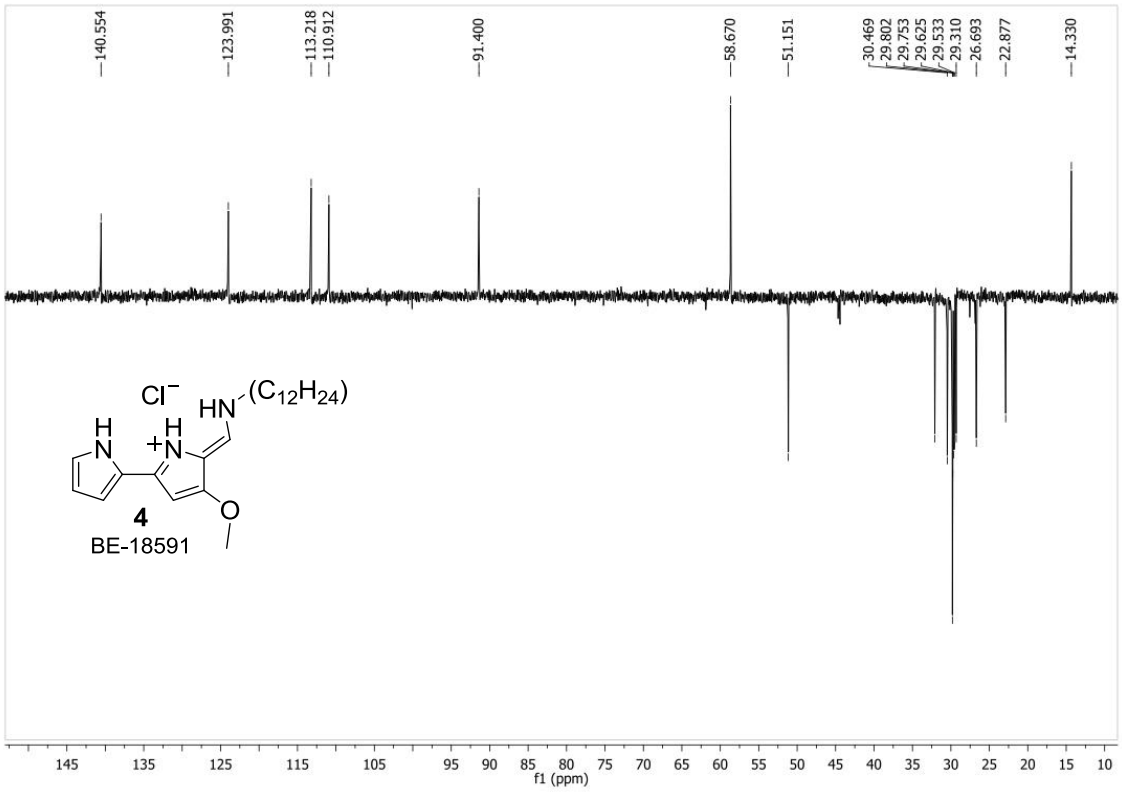

Figure S15. DEPT ^{13}C-NMR ($CDCl_3$, 75 MHz) of compound **4**.HCl.

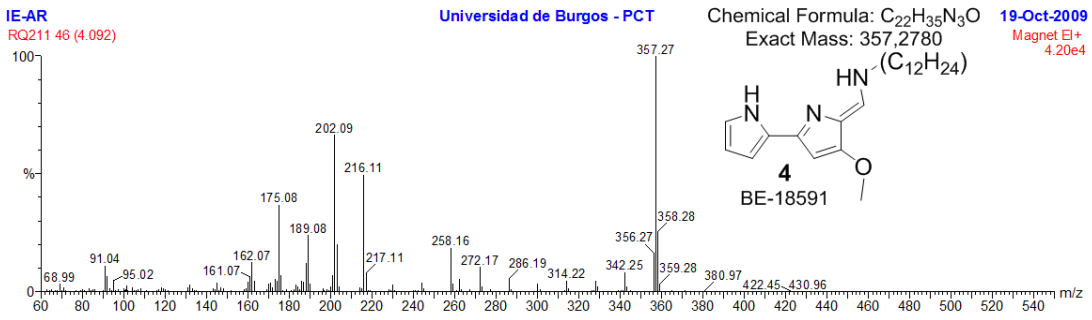

Figure S16. HRMS (EI) of compound **4**.

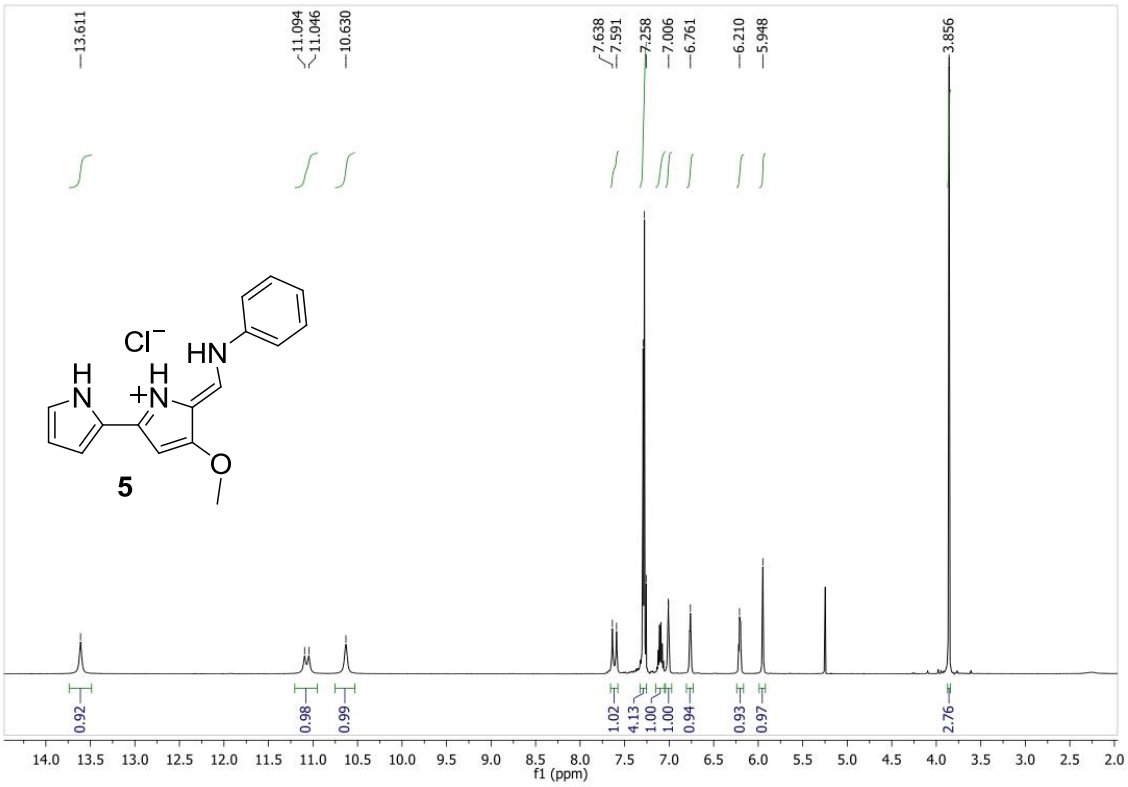

Figure S17. ^{1}H-NMR ($CDCl_3$, 300MHz)of compound **5**.HCl.

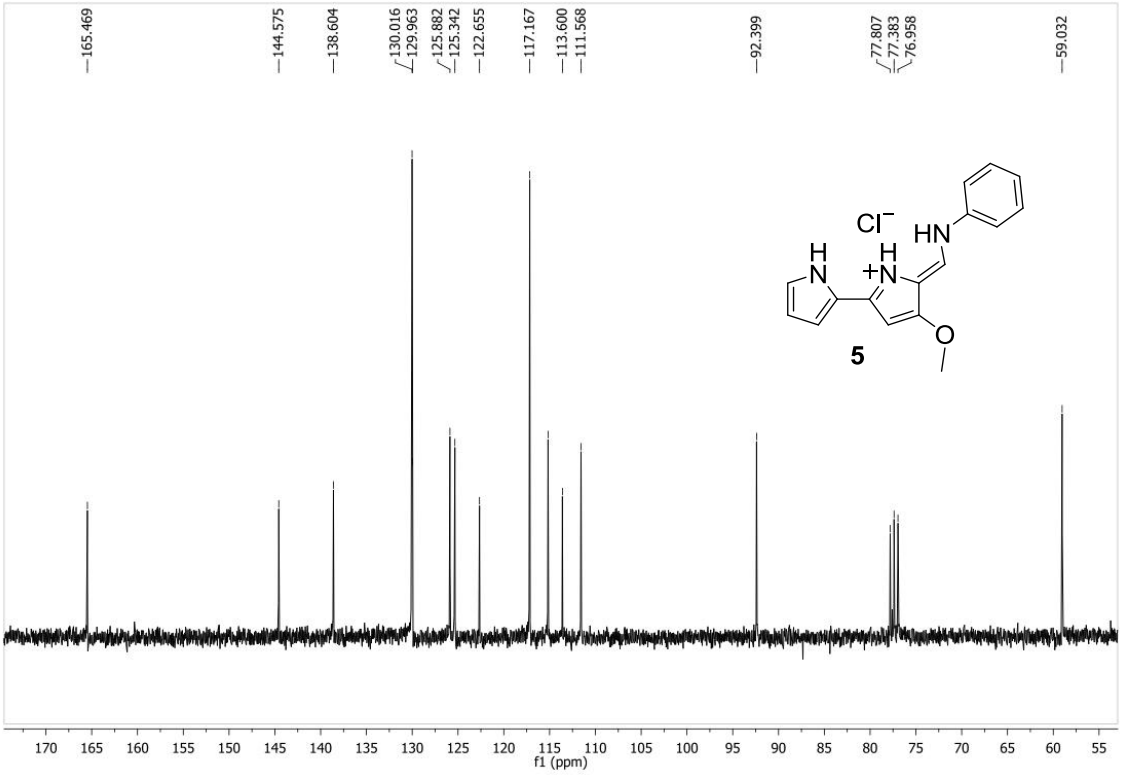

Figure S18. ^{13}C-NMR ($CDCl_3$, 75 MHz) of compound **5**.HCl.

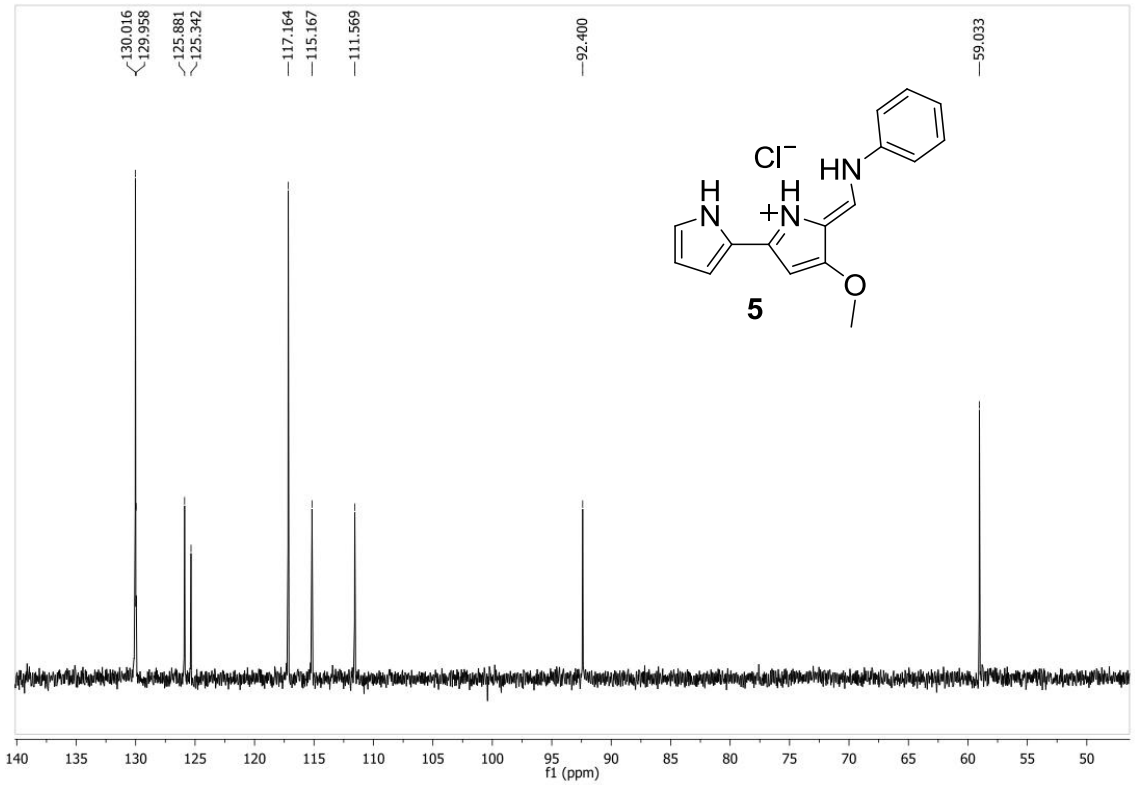

Figure S19. ^{13}C-NMR DEPT ($CDCl_3$, 75 MHz) of compound **5**.HCl.

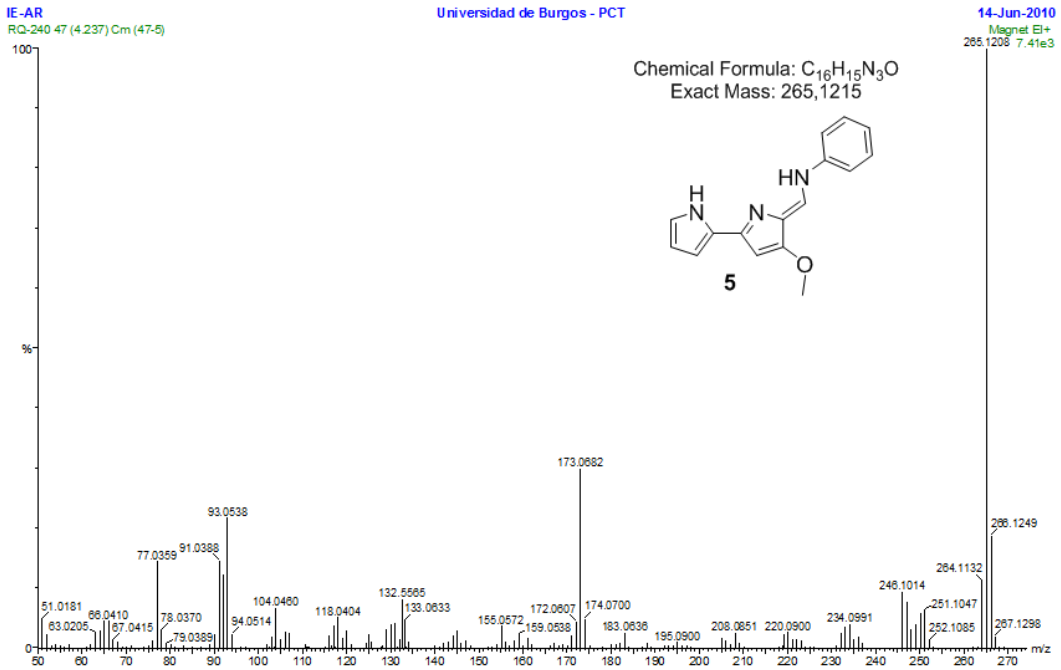

Figure S20. HRMS (EI) of compound **5**.

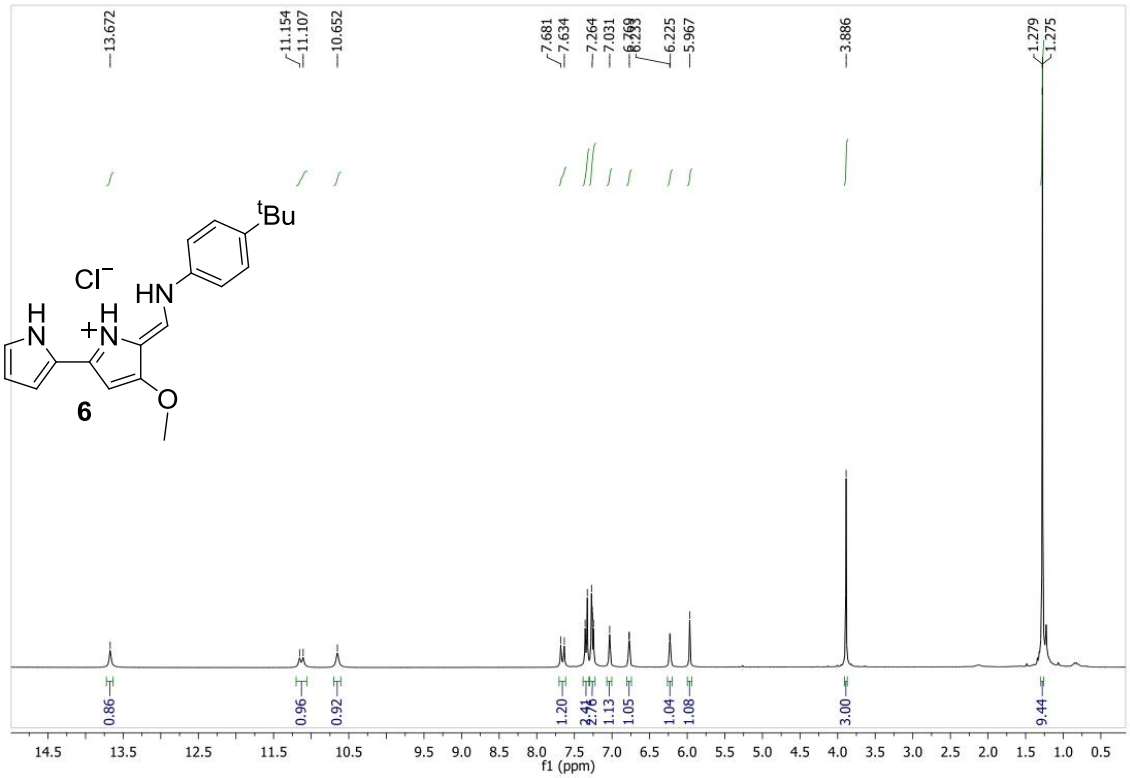

Figure S21. ^{1}H-NMR ($CDCl_3$, 300MHz) of compound **6**.HCl.

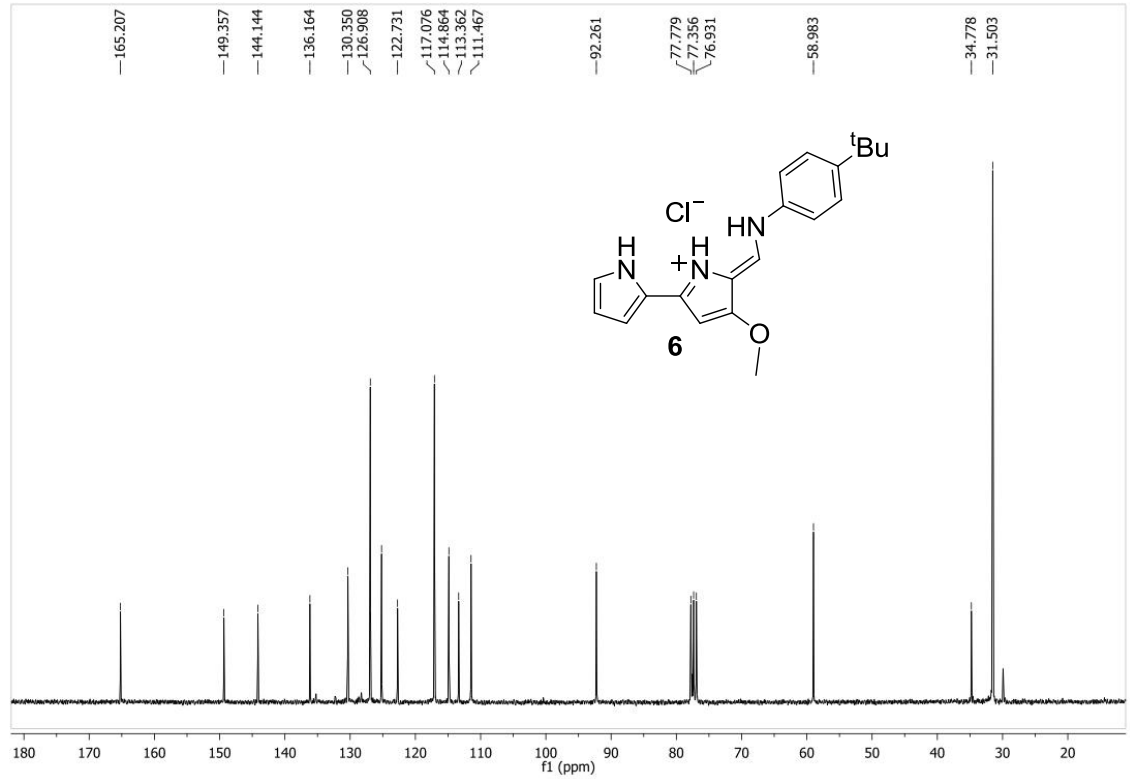

Figure S22. ^{13}C-NMR ($CDCl_3$, 75 MHz) of compound **6**.HCl.

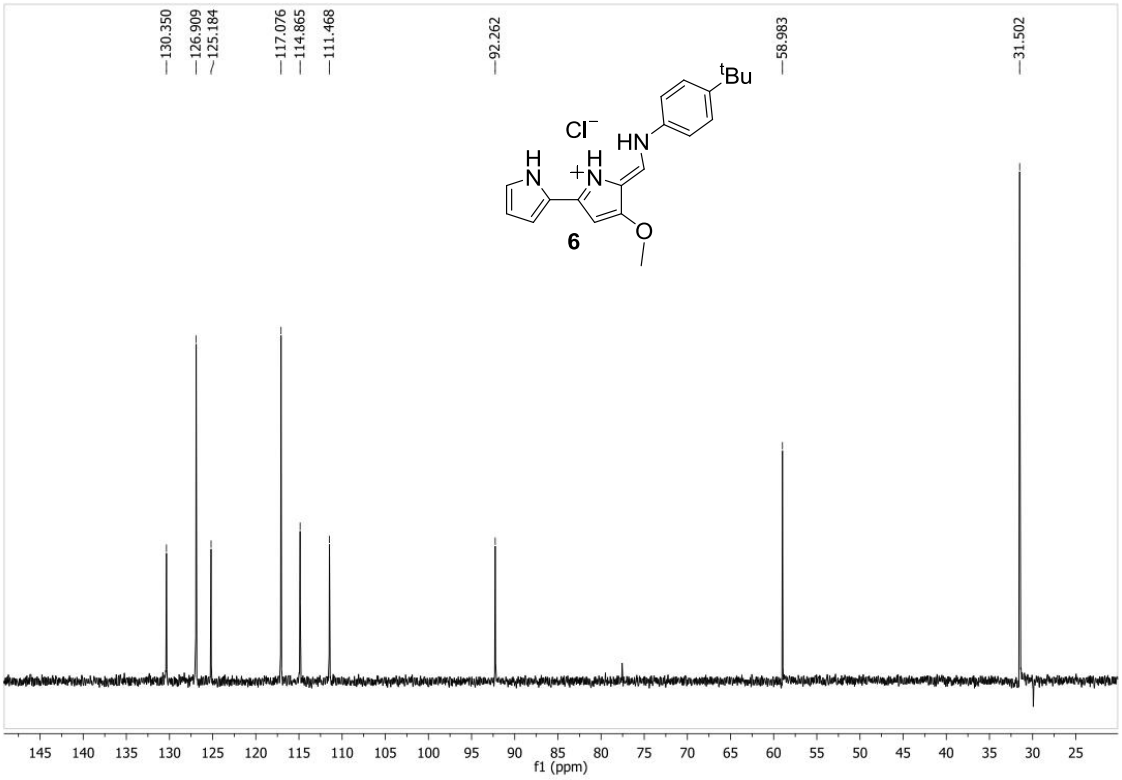

Figure S23. ^{13}C-NMR DEPT ($CDCl_3$, 75 MHz) of compound **6**.HCl.

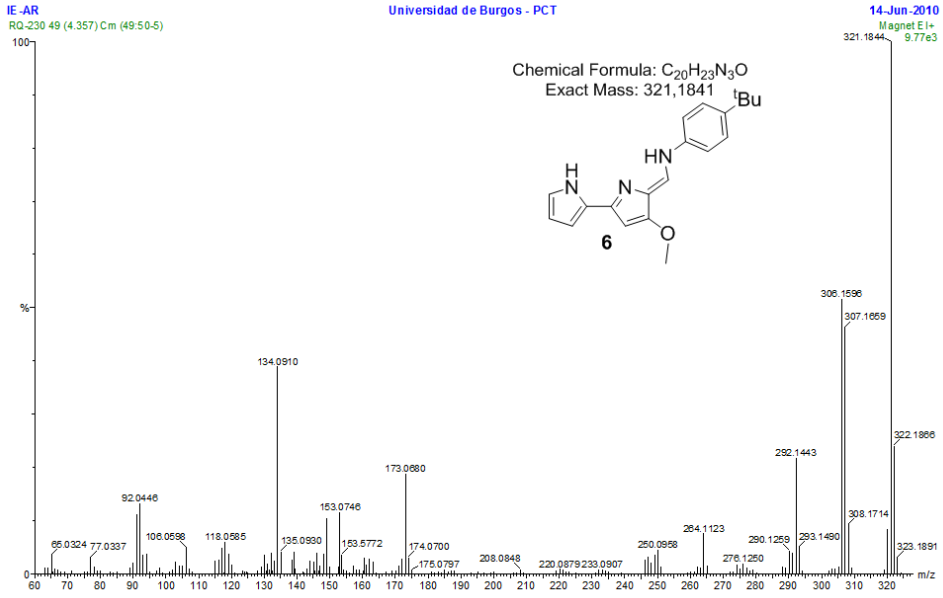

Figure S24. HRMS (EI) of compound **6**.

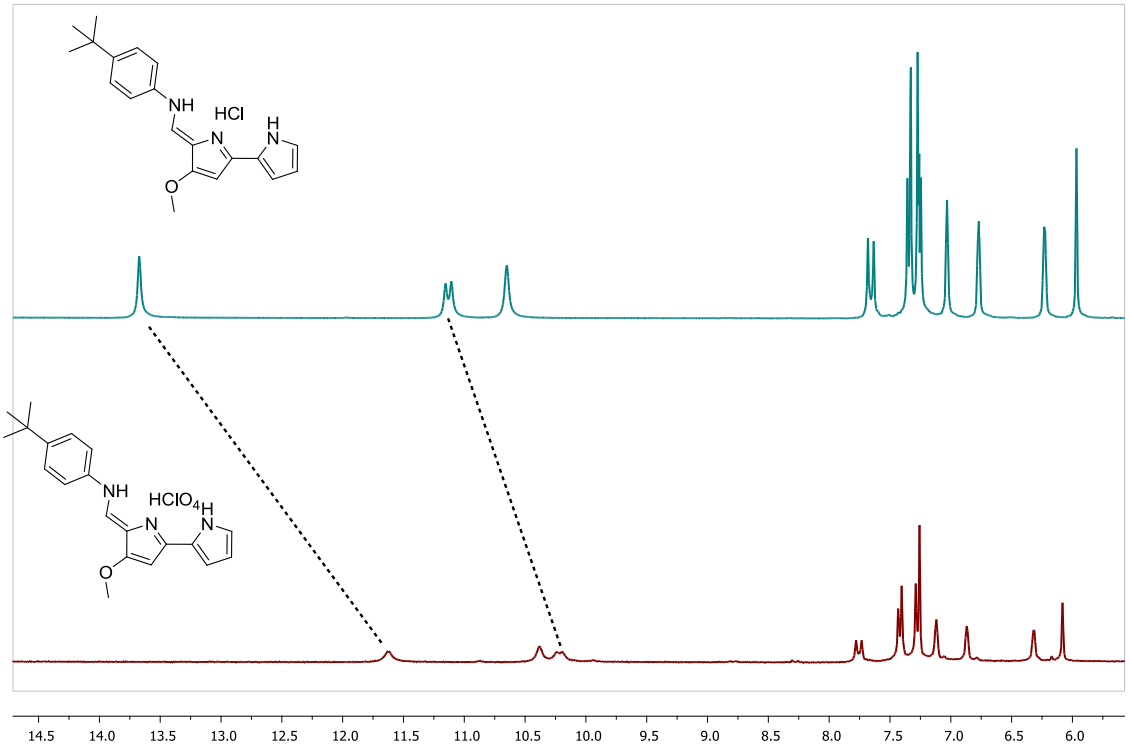

Figure S25. Comparison of ^{1}H-NMR ($CDCl_3$, 300MHz) of compound **6**.HCl and **6**.$HClO_4$ (upfield region).

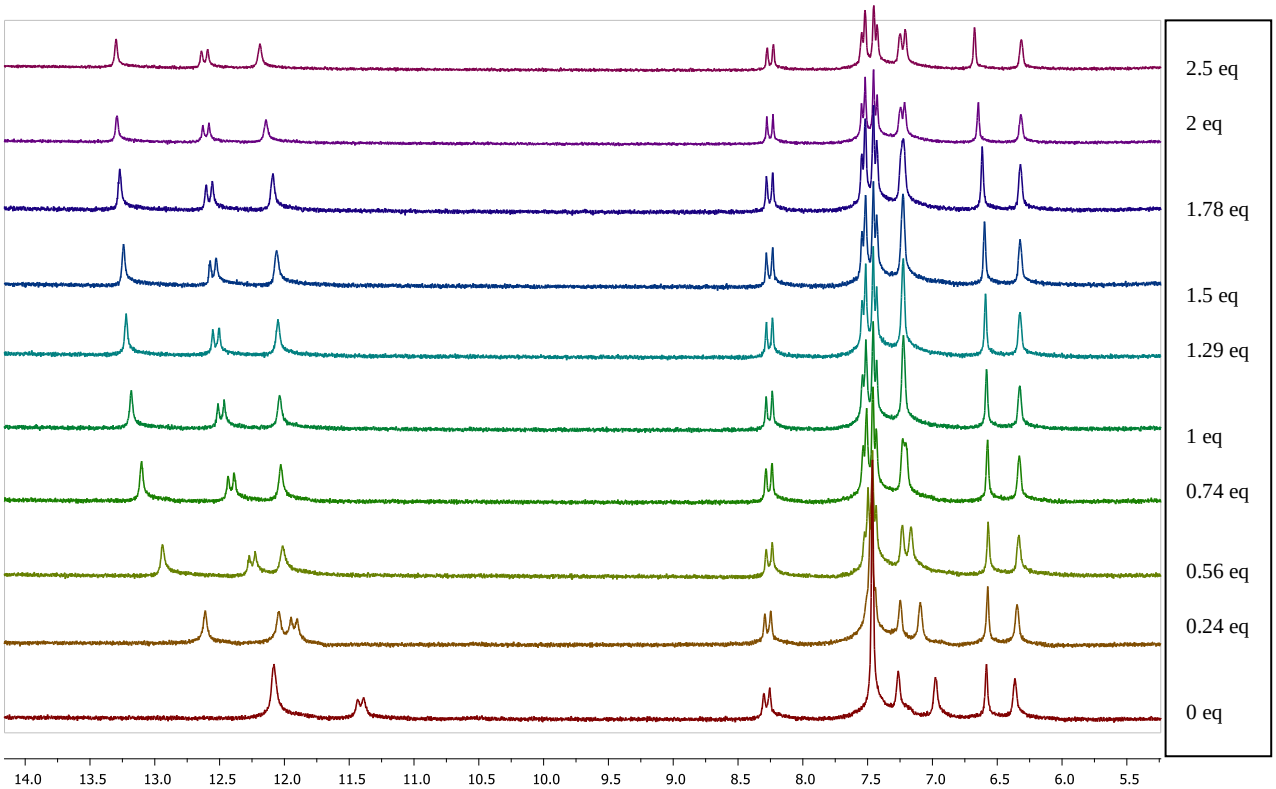

Figure S26. Stack plot of ^{1}H-NMR (d6-DMSO, 300MHz) of compound **6**.$HClO_4$ upon addition of increasing ammounts of TBACl (upfield region).

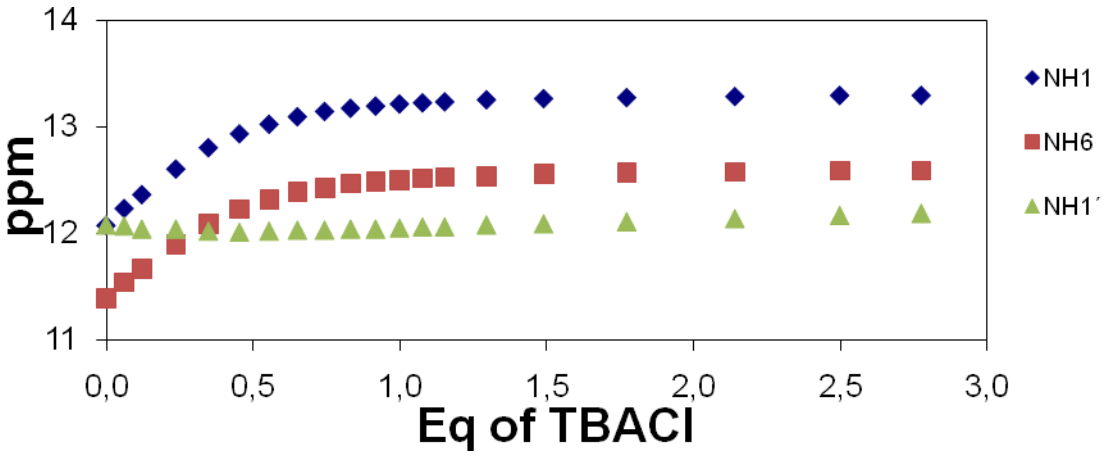

Figure S27. Movements of the NH chemical shift (d6-DMSO) of compound **6**.$HClO_4$ upon addition of increasing ammounts of TBACl. Following the changes in the chemical shifts as a function of the concentration of anion resulted in a steep curve up to one equivalent, preventing the calculation of an apparent stability constant

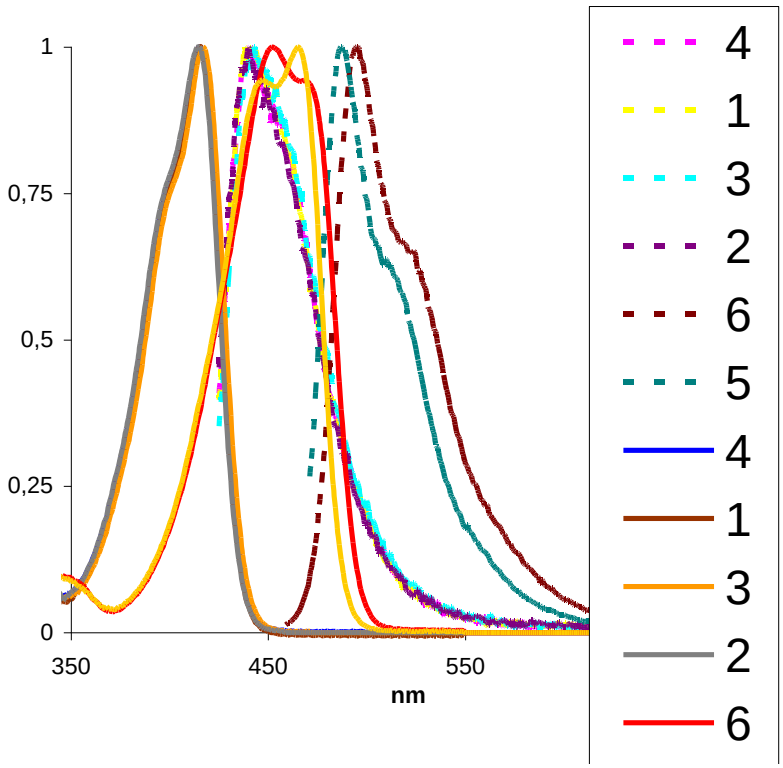

Figure S28. Normalized absorption (solid lines) and emission (dashed lines) spectra of compounds **1**-**6**) in $CHCl_3$ (10^{-5} M).

Single crystal X-ray diffraction analysis:

(CCDC 804441 (**2**) and 804442 (**6**) contain the supplementary crystallographic information for this paper. These data can be obtained free of charge from the Cambridge Crystallographic Data Centre via www.ccdc.cam.ac.uk/data_request/cif.
Single crystals of **2** and **6** were coated in **high-vacuum grease** and mounted on a glass fibre. X-ray measurements were made using a Bruker SMART CCD area-detector diffractometer with Mo-K_α radiation (λ = 0.71073 Å). Beam size 0.5. Intensities were integrated from several series of exposures, each exposure covering 0.3° in ω, and the total data set being a hemisphere. Absorption corrections were applied, based on multiple and symmetry-equivalent measurements. The structure was solved by direct methods and refined by least squares on weighted F^2 values for all reflections.

Selected crystallographic data for **2**: C12H18ClN3O2, M=271.14, Monoclinic, C2/c, a=19.739(5), b=7.0220(18), c=21.543(6) Å, α=90, β=108.563(4), γ= 90º , V=2830.8(13) Å3, Z=8; 12247reflections measured, 2491 independent (Rint=0.0278); R1(I>2σ(I))=0.0610, wR2=0.1871 (all data);
Selected crystallographic data for **6**: C20H26ClN3O2, M=375.89, Monoclinic, P2(1)/n, a=14.720(5), b=6.994(5), c=21.180(5) Å, α=90.000(5), β=108.909(5), γ= 90.000º , V=2062.8(17) Å3, Z=4; 19322reflections measured, 3630 independent (Rint=0.0328); R1(I>2σ(I))=0.0448, wR2=0.1204 (all data).

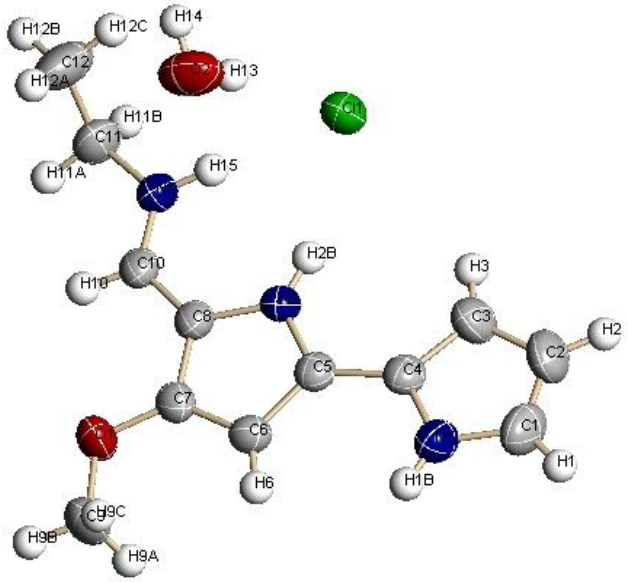

Figure S29: ORTEP diagram (50 % probability level) of the molecular structure of **2**.

Table S1. Hydrogen bonds for **2**.

D-H...A	d(D-H)	d(H...A)	d(D...A)	<(DHA)
N(3)-H(15)...Cl(1)	0.91(2)	2.32(2)	3.228(2)	173(2)
O(2)-H(14)...Cl(1)#1	0.84(4)	2.34(4)	3.161(2)	166(4)
O(2)-H(13)...Cl(1)	0.84(3)	2.37(3)	3.201(3)	167(3)
N(2)-H(2B)...Cl(1)	0.86	2.35	3.1815(17)	163.2
N(1)-H(1B)...O(2)#2	0.86	2.01	2.868(3)	176.7

Symmetry transformations used to generate equivalent atoms:

#1 -x+1/2,y+1/2,-z+1/2 #2 -x+1/2,-y+3/2,-z

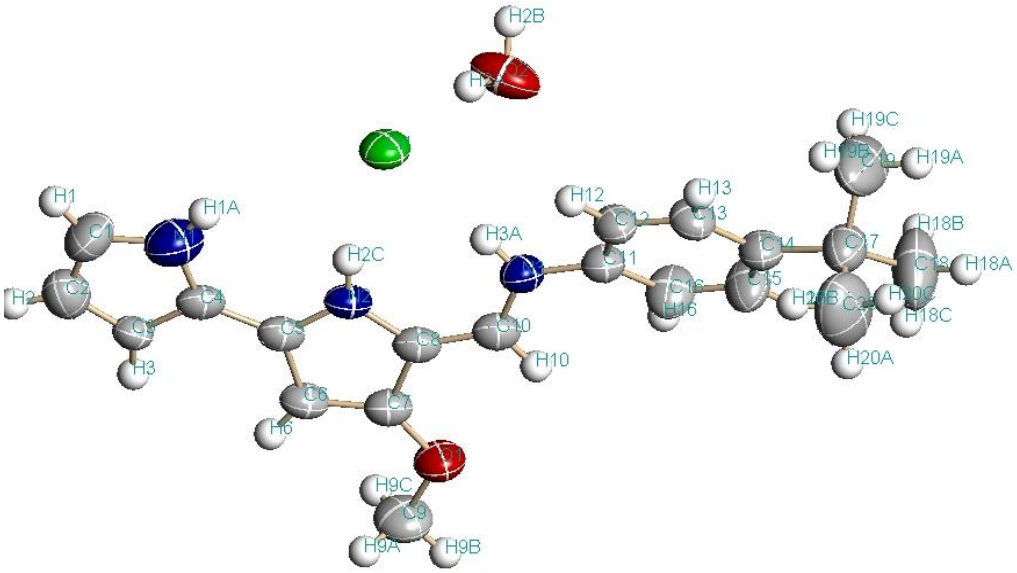

Figure S30: ORTEP diagram (50 % probability level) of the molecular structure of **6**.

Table S2. Hydrogen bonds for **6**.

D-H...A	d(D-H)	d(H...A)	d(D...A)	<(DHA)
O(2)-H(2B)...Cl(1)#1	0.908(19)	2.33(2)	3.223(3)	168(4)
O(2)-H(2A)...Cl(1)	0.933(19)	2.26(2)	3.166(3)	163(4)
N(3)-H(3A)...Cl(1)	0.86	2.35	3.210(2)	178.2
N(2)-H(2C)...Cl(1)	0.86	2.34	3.183(2)	165.6
N(1)-H(1A)...Cl(1)	0.86	3.23	3.996(4)	149.0

Symmetry transformations used to generate equivalent atoms:

#1 -x+1/2,y+1/2,-z+3/2

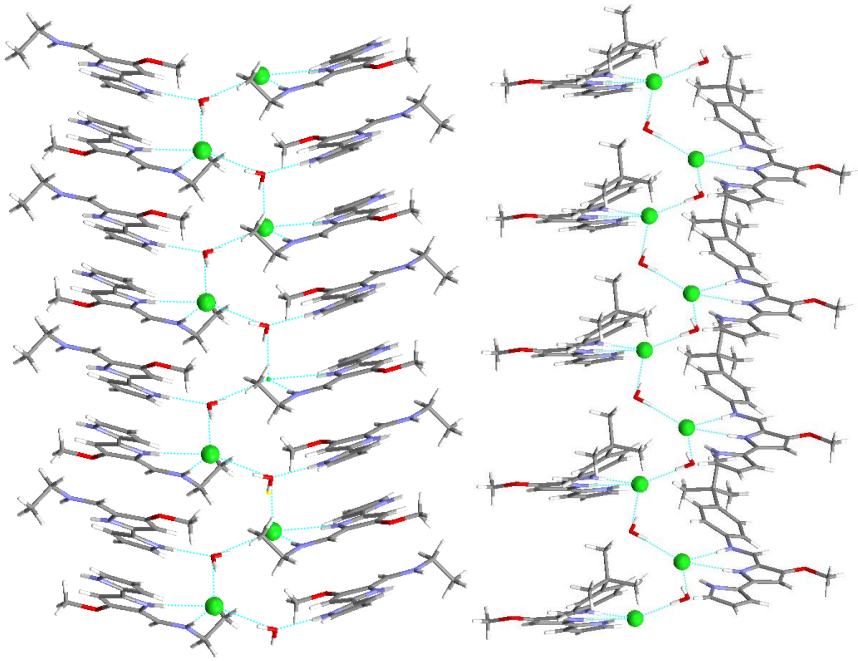

Figure S31: Representation of the solid state structures of compounds **2** (left) and **6** (right). These structures with stacked receptors forming channels filled with chloride and water molecules resemble that proposed recently by Gokel and colleagues for dipicolil dianilides.[3]

Preparation of Phospholipid Vesicles. A chloroform solution of 1-palmitoyl-2-oleoyl-*sn*-glycero-3-phosphocholine (POPC) (20 mg/mL) (Sigma-Aldrich) was evaporated *in vacuo* using a rotary evaporator and the lipid film obtained was dried under high vacuum for at least 2 hours. The lipid film was rehydrated by addition of a sodium chloride solution (451 mM NaCl and 20 mM phosphate buffer, pH 7.2 or 476 mM NaCl and 10 mM phosphate buffer, pH 7.2 or 498 mM NaCl and 20 mM MES buffer, pH 5.3) and followed by careful vortexing. The lipid suspension was then subjected to nine freeze-thaw cycles and twenty-nine extrusions through a 200 nm polycarbonate Nucleopore membrane using a LiposoFast Basic extruder (Avestin, Inc.). The resulting unilamellar vesicles were dialyzed against Na_2SO_4 solution (150 mM Na_2SO_4 and 20 mM phosphate buffer, pH 7.2 or 166 mM Na_2SO_4 and 20 mM MES buffer, pH 5.3) or a $NaNO_3$ solution (476 mM $NaNO_3$ and 10 mM phosphate buffer, pH 7.2) to remove unencapsulated chloride.

ISE Transport Assays. Unilamellar vesicles (200 nm mean diameter) composed of POPC containing an encapsulated solution of 451 mM NaCl and 20 mM phosphate buffer, pH 7.2 or 498 mM NaCl and 20 mM MES buffer, pH 5.3, were suspended in a solution 150 mM Na_2SO_4 and 20 mM phosphate buffer, pH 7.2 or 160 mM Na_2SO_4 and 20 mM MES buffer, pH 7.2 respectively, for a final lipid concentration of 0.5 mM and a total volume of 5 mL. A DMSO solution of the carrier molecule, typically 5 µL to avoid influence of the solvent molecules in the assay, was added and the chloride release from vesicles was monitored using a sympHony chloride selective electrode. At the end of the experiment the vesicles were lysed with detergent (triton-X 10% dispersion in water, 60 µL) to release all chloride ions; the resulting value was considered to represent 100% release and used as such. For the bicarbonate anion exchange assays to the vesicles suspended in a Na_2SO_4 solution a solution of $NaHCO_3$ (500 mM in Na_2SO_4 buffered to pH 7.2 with 20 mM sodium phosphate salts) was added for a final concentration of 40 mM and the chloride efflux was monitored for another 5 minutes before they were lysed with detergent to release all chloride ions; the resulting value was considered to represent 100% release and used as such. For the experiments using $NaNO_3$ as external solution vesicles containing an encapsulated solution of 451 mM NaCl and 20 mM phosphate buffer, were suspended in a 476 mM $NaNO_3$ and 10 mM phosphate buffer, pH 7.2 solution.

[3] C. R. Yamnitz, S. Negin, I. A. Carasel, R. K. Winter and G. W. Gokel, *Chem. Commun.*, 2010, **46**, 2838.

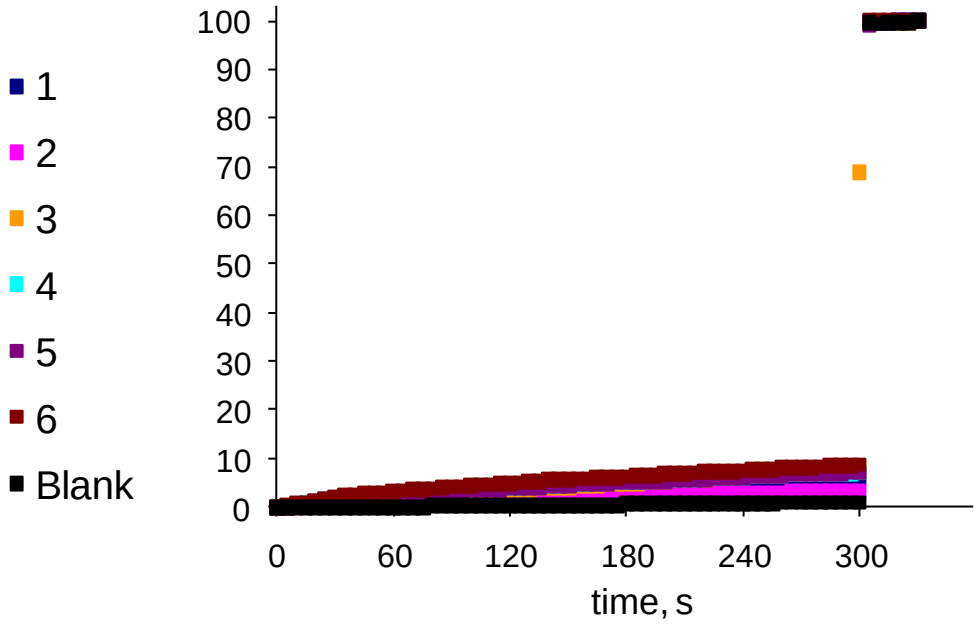

Figure S32: Chloride efflux upon addition of **1**-**6** (1 μM, 0.2 % molar carrier to lipid) to vesicles composed of POPC. The vesicles contained NaCl (451 mM NaCl and 20 mM phosphate buffer, pH 7.2) and were immersed in Na_2SO_4 (150 mM Na_2SO_4 and 20 mM phosphate buffer, pH 7.2). At the end of the experiment the vesicles were lysed with detergent to release all chloride ions and the resulting value was considered to represent 100% release and used as such. Each trace represents the average value of three independent experiments.

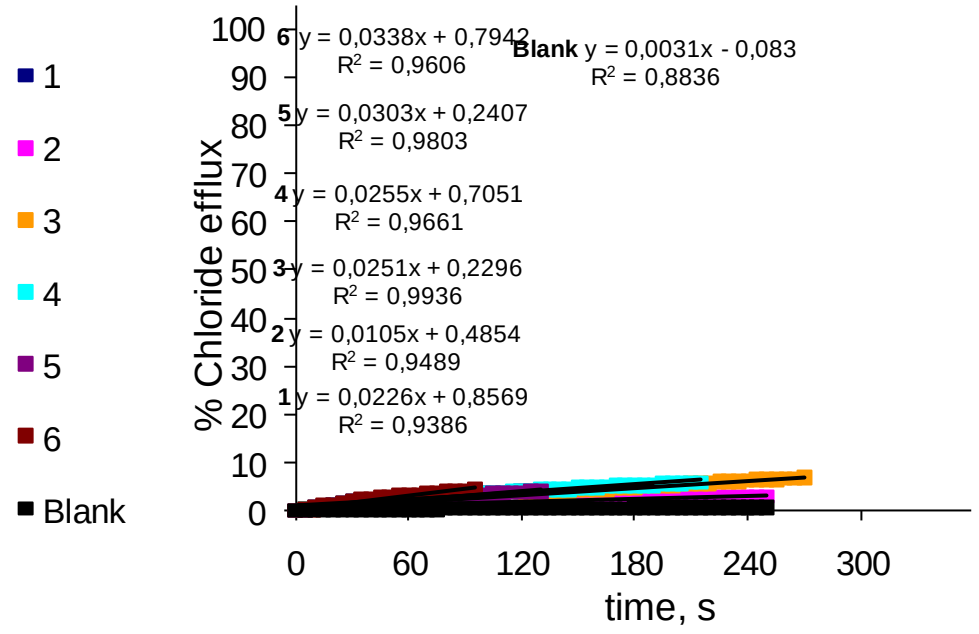

Figure S33: Fitting of the initial slope resulting from the chloride efflux promoted by **1**-**6** under the conditions described in S32 used for comparative purposes.

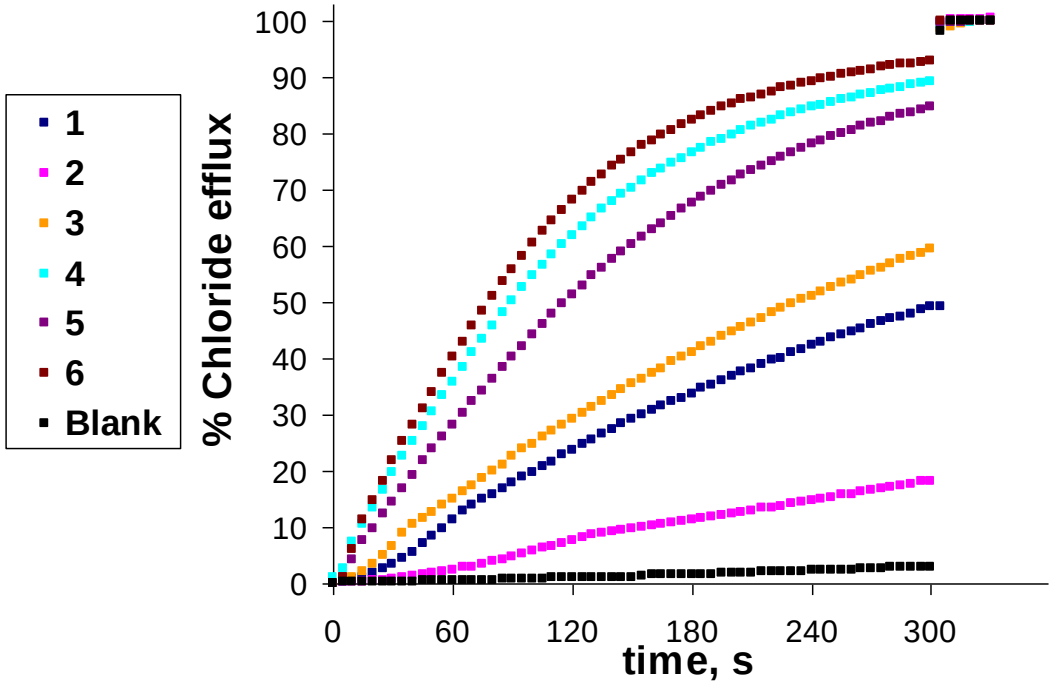

Figure S34: Chloride efflux upon addition of **1**-**6** (1 μM, 0.2 % molar carrier to lipid) to vesicles composed of POPC. The vesicles contained NaCl (451 mM NaCl and 20 mM phosphate buffer, pH 7.2) and were immersed in Na_2SO_4 (150 mM Na_2SO_4 and 20 mM phosphate buffer, pH 7.2). At t=0 a $NaHCO_3$ solution to (500 mM in Na_2SO_4 buffered to pH 7.2 with 20 mM sodium phosphate salts) was added for a final concentration of 40 mM and the chloride efflux was monitored for 5 minutes. The vesicles were lysed with detergent to release all chloride ions and the resulting value was considered to represent 100% release and used as such. Each trace represents the average value of three independent experiments.

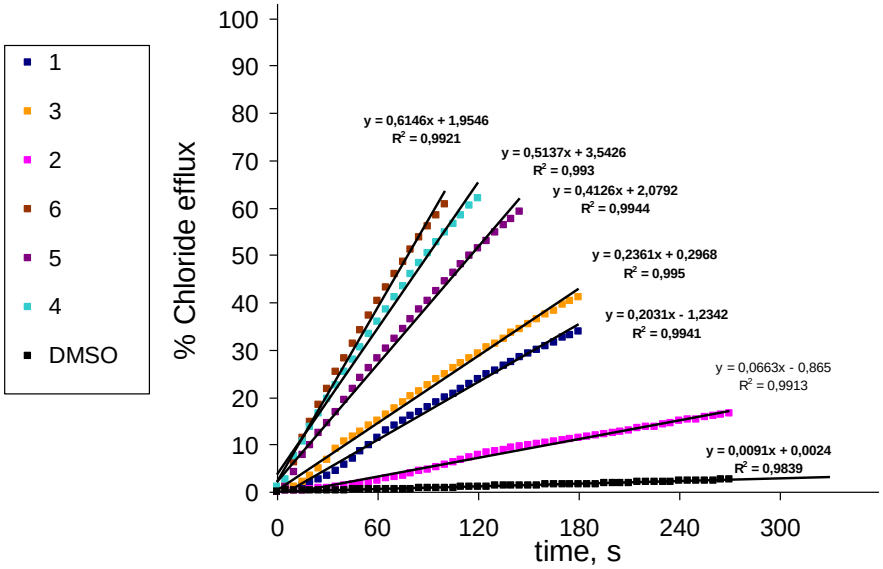

Figure S35: Fitting of the initial slope resulting from the chloride efflux promoted by **1**-**6** under the conditions described in S34 used for comparative purposes.

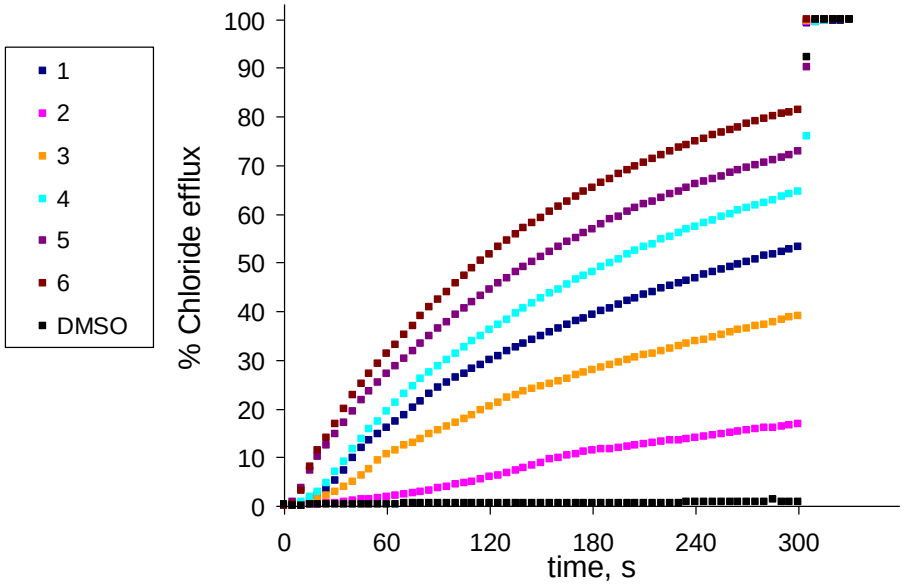

Figure S36: Chloride efflux upon addition of **1**-**6** (0.1 μM, 0.02 % molar carrier to lipid) to vesicles composed of POPC. The vesicles contained NaCl (476 mM NaCl and 10 mM phosphate buffer, pH 7.2) and were immersed in $NaNO_3$ (476 mM $NaNO_3$ and 10 mM phosphate buffer, pH 7.2). Once the electrode reading was stable the carrier was added and the chloride efflux was monitored for 5 minutes. At the end of the experiment the vesicles were lysed with detergent to release all chloride ions and the resulting value was considered to represent 100% release and used as such.

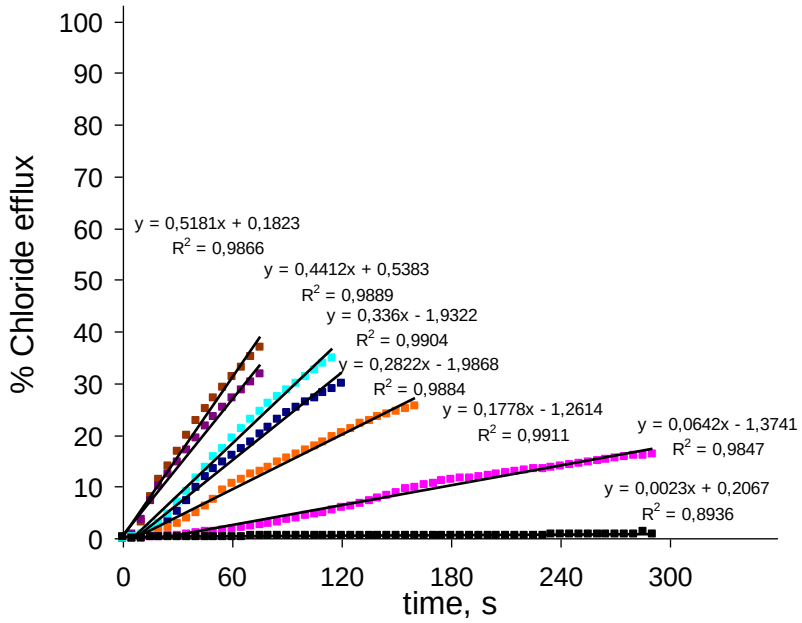

Figure S37: Fitting of the initial slope resulting from the chloride efflux promoted by **1**-**6** under the conditions described in S36 used for comparative purposes.

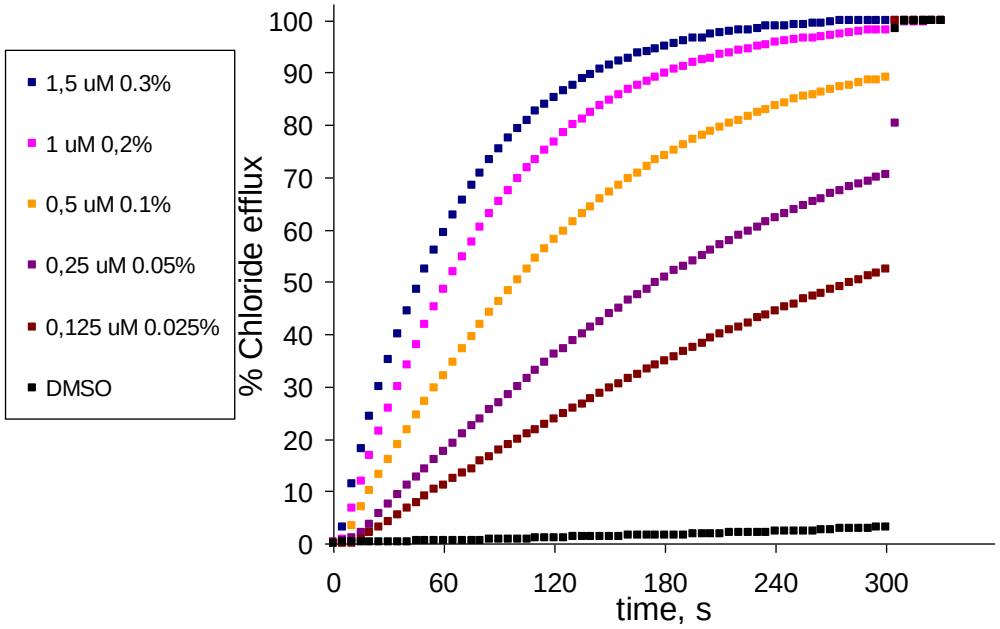

Figure S38: Chloride efflux upon addition of **6** (1.5-0.125 μM, 0.3-0.025 % molar carrier to lipid) to vesicles composed of POPC. The vesicles contained NaCl (451 mM NaCl and 20 mM phosphate buffer, pH 7.2) and were immersed in Na_2SO_4 (150 mM Na_2SO_4 and 20 mM phosphate buffer, pH 7.2). At t=0 a $NaHCO_3$ solution to (500 mM in Na_2SO_4 buffered to pH 7.2 with 20 mM sodium phosphate salts) was added for a final concentration of 40 mM and the chloride efflux was monitored for 5 minutes. The vesicles were lysed with detergent to release all chloride ions and the resulting value was considered to represent 100% release and used as such.

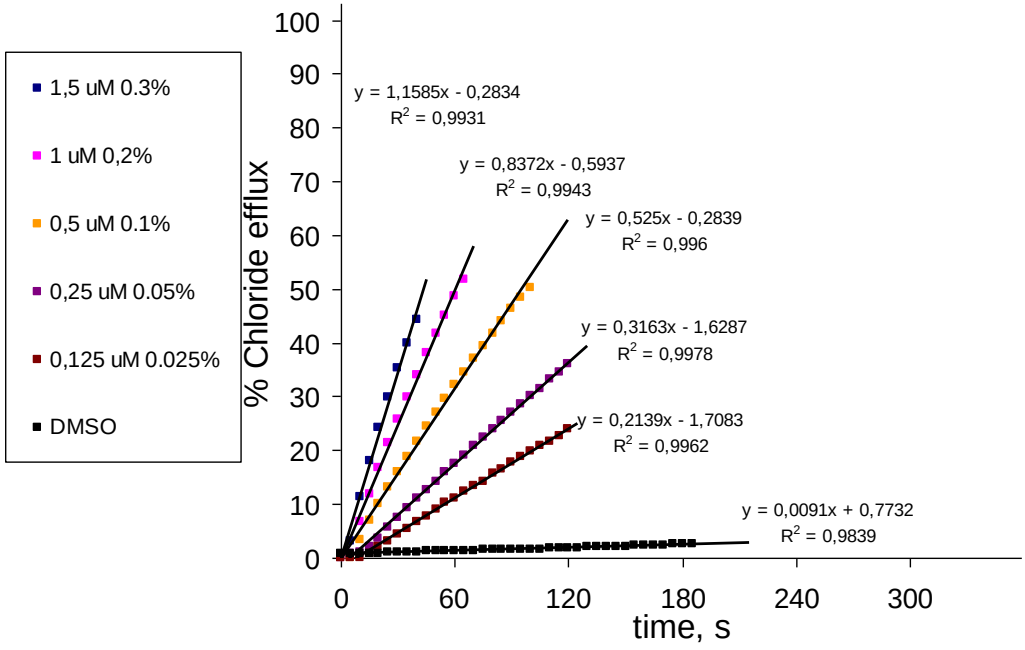

Figure S39: Fitting of the initial slope resulting from the chloride efflux promoted by different concentrations of **6** under the conditions described in S38 used for comparative purposes.

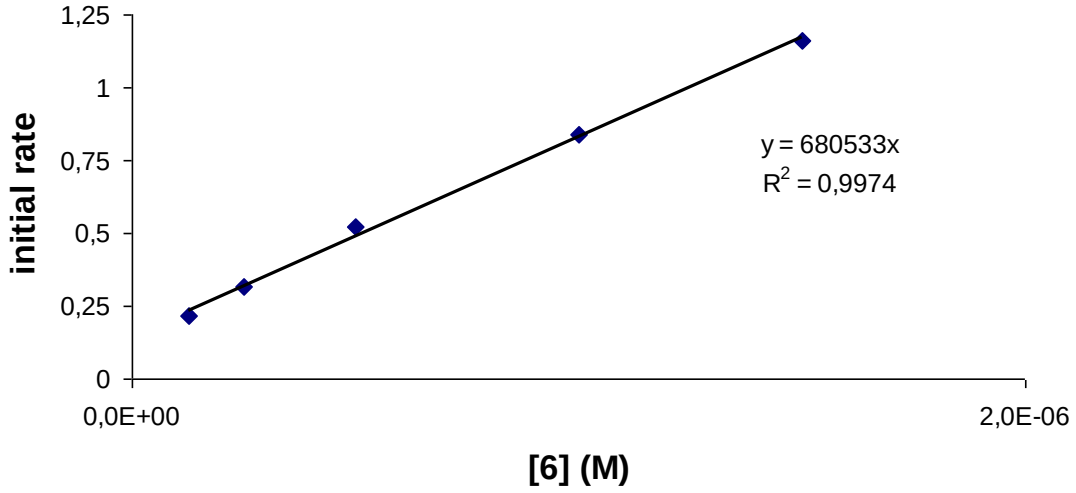

Figure S40: Plot of the initial rate ($\%s^{-1}$) vs concentration of **6** (M) under the conditions described in S38 and S39 showing the linear dependence in the range analyzed.

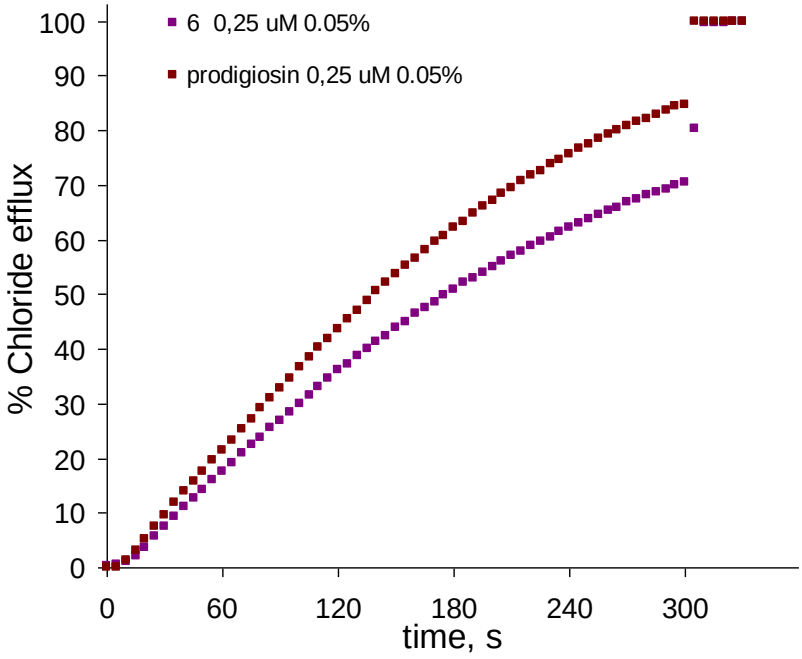

Figure S41: Chloride efflux upon addition of **6** and prodigiosin (0.25 μM, 0.05 % molar carrier to lipid) to vesicles composed of POPC. The vesicles contained NaCl (451 mM NaCl and 20 mM phosphate buffer, pH 7.2) and were immersed in Na_2SO_4 (150 mM Na_2SO_4 and 20 mM phosphate buffer, pH 7.2). At t=0 a $NaHCO_3$ solution to (500 mM in Na_2SO_4 buffered to pH 7.2 with 20 mM sodium phosphate salts) was added for a final concentration of 40 mM and the chloride efflux was monitored for 5 minutes. The vesicles were lysed with detergent to release all chloride ions and the resulting value was considered to represent 100% release and used as such.

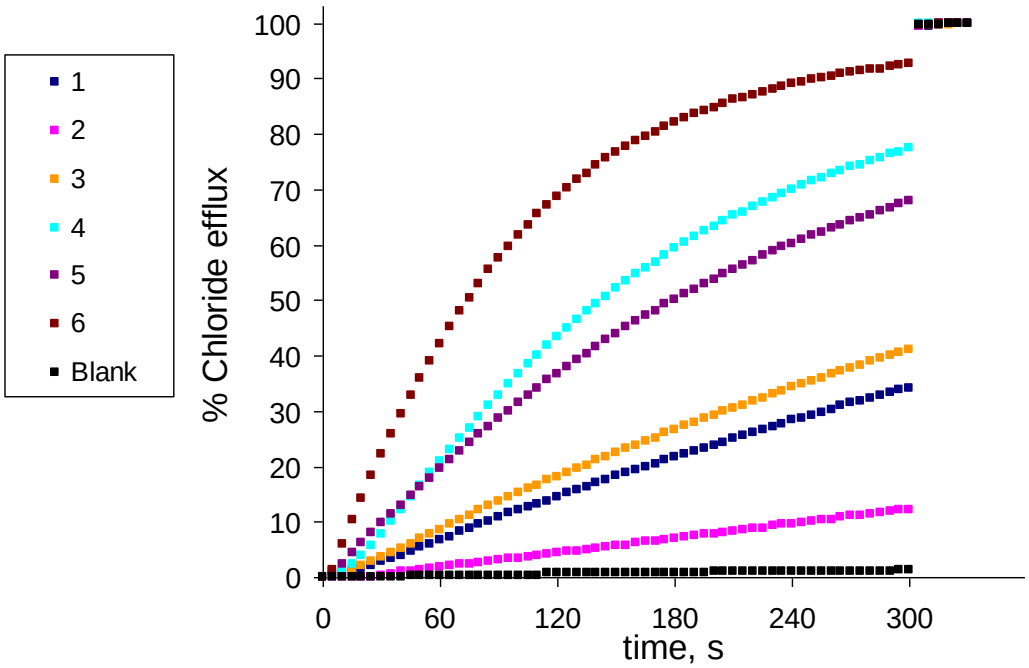

Figure S42: Chloride efflux upon addition of **1**-**6** (1 μM, 0.2 % molar carrier to lipid) to vesicles composed of POPC. The vesicles contained NaCl (468 mM NaCl and 20 mM MES buffer, pH 5.3) and were immersed in Na_2SO_4 (160 mM Na_2SO_4 and 20 mM MES buffer, pH 7.2). At t=0 a $NaHCO_3$ solution to (500 mM in Na_2SO_4 buffered to pH 7.2 with 20 mM MES) was added for a final concentration of 40 mM and the chloride efflux was monitored for 5 minutes. The vesicles were lysed with detergent to release all chloride ions and the resulting value was considered to represent 100% release and used as such.

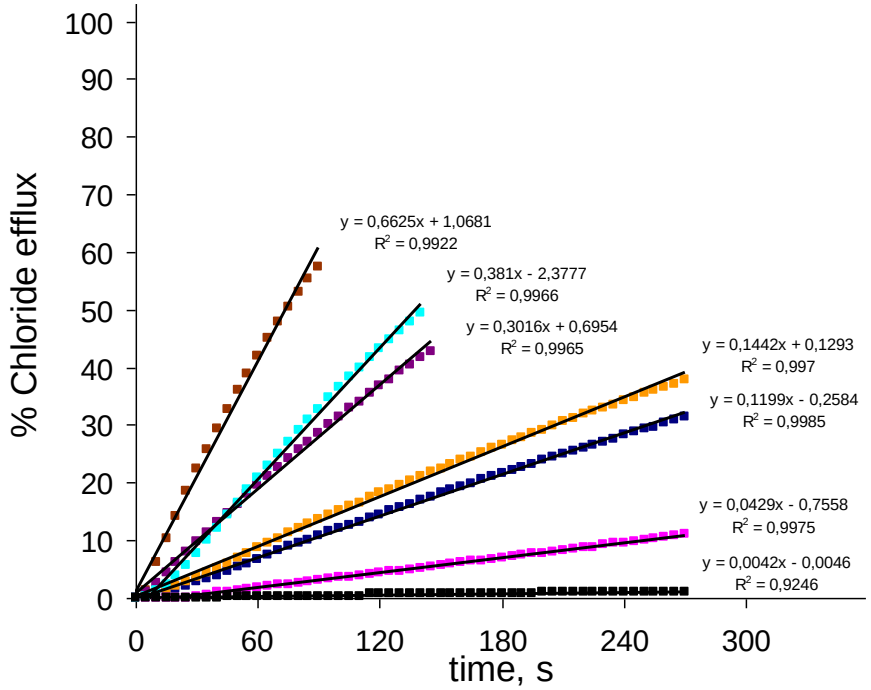

Figure S43: Fitting of the initial slope resulting from the chloride efflux promoted by **1**-**6** under the conditions described in S42 used for comparative purposes.

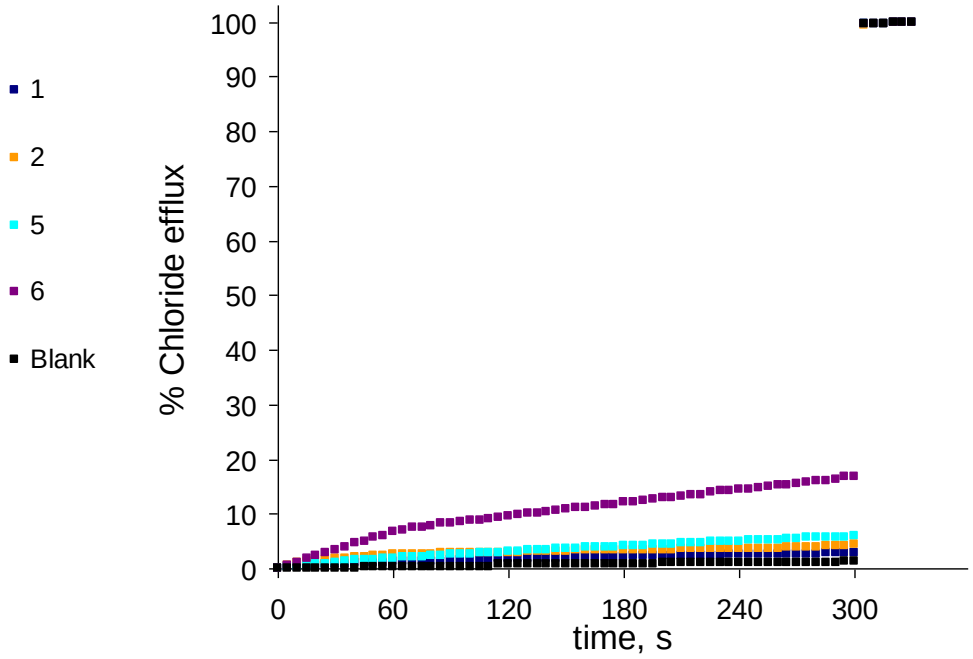

Figure S44: Chloride efflux upon addition of **1**-**6** (1 μM, 0.2 % molar carrier to lipid) to vesicles composed of POPC. The vesicles contained NaCl (468 mM NaCl and 20 mM MES buffer, pH 5.3) and were immersed in Na_2SO_4 (160 mM Na_2SO_4 and 20 mM MES buffer, pH 7.2). The chloride efflux was monitored for 5 minutes and then the vesicles were lysed with detergent to release all chloride ions and the resulting value was considered to represent 100% release and used as such.

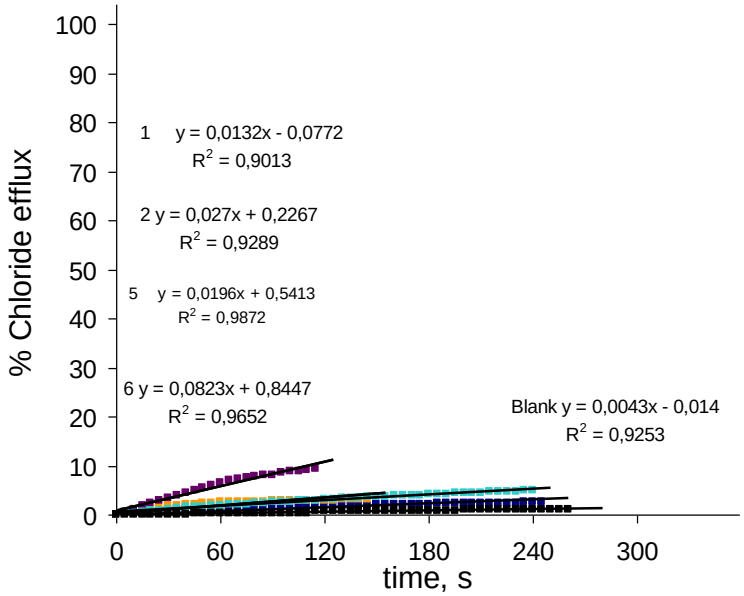

Figure S45: Fitting of the initial slope resulting from the chloride efflux promoted by **1**-**6** under the conditions described in S44 used for comparative purposes.

Cell Culture MATERIAL AND METHODS

Human small cells lung cancer cell line (GLC4) were cultured in RPMI 1640 medium (Biological Industries, Beit Haemek, Israel), supplemented with10% FBS, 100 U/ml penicillin, 100 μg/ml streptomycin (all from GIBCO BRL, Paisley, UK), and 2 mM L-glutamine (Sigma Chemicals Co, St Louis, MO, USA), at 37 ºC, 5% CO_2 in air.

Vital fluorescence microscopy

The living cultured cells were stained with acridina orange (AO) (Holtzman, 1989). Briefly, cells on a chamber slide were incubated without and with 800nM of the tambjamines compounds **1**-**6** in RPMI supplemented with 10% FBS at 37 ºC for 15 min. to 1h. After 3 washed with PBS cells were incubated with 5 µg/ml AO in PBS for 30 min. The chamber slides were washed 3 times with PBS solution supplemented with 10% FBS and then examined with a Nikon microscope (E800) and photographed with diagnostic instruments photo automat system (Spot JR).

REFERENCES

A.Allison, A.C., Young, M.R., 1969. In: Dingle, J.T., Fell, H.B. (Eds.),Lysosomes in Biology and Pathology, vol. 2, pp. 600–628.

Mosmann, T. Rapid colorimetric assay for cellular growth and survival: application for proliferation and citotoxicity assy. J. Inmunol. Mehods 1983, 65:55-63.

Holtzman, E., 1989. Lysosomes. Plenum Press, New York, pp. 95– 100.